Energy Policy 88 (2016) 371–388

Contents lists available at ScienceDirect

Energy Policy

journal homepage: www.elsevier.com/locate/enpol

Robust resource adequacy planning in the face of coal retirements

Roger Lueken [a,*], Jay Apt [a,b], Fallaw Sowell [b]

[a] Department of Engineering and Public Policy, Carnegie Mellon University, Pittsburgh, PA 15213, USA
[b] Tepper School of Business, Carnegie Mellon University, Pittsburgh, PA 15213, USA

HIGHLIGHTS

- We model resource adequacy in the PJM Interconnection.
- If plant failures are independent, PJM could retire 11 GW of "at-risk" coal.
- If plant failures are correlated, risks of supply shortages may be high.

ARTICLE INFO

Article history:
Received 2 May 2015
Received in revised form
13 September 2015
Accepted 19 October 2015

Keywords:
Resource adequacy
Capacity planning
Risk
Statistical modeling
Market design

ABSTRACT

We investigate the resource adequacy requirements of the PJM Interconnection, and the sensitivity of capacity procurement decisions to the choice of reliability metric used to measure resource adequacy. Assuming that plants fail independently, we find that PJM's 2010 reserve margin of 20.5% was sufficient to achieve the stated reliability standard of one loss of load event per ten years, with 0.012 expected loss of load events per year. PJM could reduce reserve margins to 13% and still achieve adequate levels of reliability as measured by the 2.4 Loss of Load Hours metric and the 0.001% Unserved Energy metric, which are used by other U.S. and international systems. A reserve margin of 13–15% would minimize long-run system costs. Reducing reserve margins from 20.5% to 13% in 2010 would have reduced PJM's capacity procurement by 11 GW, the same amount of coal capacity that PJM has identified as at high risk of retirement. We also investigate the risk posed by correlated failures among generators, a risk traditionally not modeled by system planners. We illustrate that three types of correlated failures may increase outage risks: natural gas supply disruptions, reduced reliability among generators during winter months, and the simultaneous shutdown of multiple nuclear generators for regulatory reasons.

© 2015 Elsevier Ltd. All rights reserved.

1. Introduction

Over the next decade, significant coal plant retirements are expected in the United States. The Energy Information Agency forecasts that 40 GW of coal capacity will retire between 2014 and 2020 (EIA, 2014). These retirements are due to a combination of factors. Many coal plants are near the end of their expected lifespan. Many small and outdated coal plants are finding it cost prohibitive to make the retrofits necessary to comply with emission regulations. Low natural gas prices have put downward pressure on revenues from wholesale electricity prices.

These retirements pose a new challenge to system operators, who are mandated to meet resource adequacy requirements. To meet these requirements, systems procure generation capacity that is rarely used but is needed in extreme circumstances. This capacity, typically natural gas combustion turbines, has low upfront capital costs but high operating costs. In the traditional regulated utility model, these generators are compensated through rate-of-return ratemaking, even if they produce no power. The restructuring of 20 U.S. states in the late 1990s and early 2000s led the industry to recognize the so-called "missing money problem", whereby market designs would not support sufficient generation investment (Joskow, 2006, 2008; Spees et al., 2013). Today, many restructured markets use capacity markets to compensate generators for the capacity they provide. Since 2007, PJM has procured capacity through its centralized capacity market. Capacity market billings were $8 billion in both the 2009/2010 and 2010/2011 auctions. In 2010, capacity costs were roughly 18% of total 2010 billings (PJM, 2011a).

Resource adequacy modeling underpins the planning decisions made in today's electricity systems. In both traditionally regulated states with Integrated Resource Planning processes and restructured states with ISO-administered capacity markets, resource adequacy models play a major role in determining the

* Corresponding author. Tel.: +1 202 419 3321.
E-mail address: Roger.Lueken@brattle.com (R. Lueken).

http://dx.doi.org/10.1016/j.enpol.2015.10.025
0301-4215/© 2015 Elsevier Ltd. All rights reserved.

amount of capacity that is built. These models consider the reliability of existing generators and forecasts of load. Both generator outages and load forecasts are highly uncertain, creating the risk that inaccurate modeling may lead to an over- or under-procurement of capacity. Over-procuring capacity will increase costs for ratepayers; under-procuring capacity will create outage risks above reliability targets.

The traditional metric of resource adequacy is the number of loss of load events (LOLE) per ten years. Most U.S. systems, including the PJM Interconnection, procure enough capacity to meet a LOLE standard of one expected event per ten years, or 0.1 events per year (0.1 LOLE standard) (PJM, 2013). The 0.1 LOLE standard dates back to the 1950s, although its origins are unknown (EISPC, 2013; Pfeifenberger et al., 2013). Here we follow the standard definition of an outage "event" as an outage lasting one or more consecutive hours. The LOLE metric is problematic, because it considers neither the duration of an outage nor the magnitude of load shed during an outage.

Instead of the LOLE metric, some systems have adopted other standards. The Southwest Power Pool (SPP) uses the metric of 24 expected loss of load hours (LOLH) per ten years, or 2.4 h per year (2.4 LOLH standard) (EISPC, 2013). The Scandinavian system uses the metric of expected unserved energy (UE) totaling 0.001% of total load served (0.001% UE standard). Australia's National Energy Market (NEM) and South West Interconnected System (SWIS) have adopted a 0.002% UE standard (Pfeifenberger et al., 2013). The North American Electric Reliability Corporation has recommended system operators adopt UE standards, as they explicitly consider the magnitude of outages (NERC, 2010). All three metrics consider only the risk of generator outages, and exclude other risks such as transmission or distributions outages.

Although a significant body of literature exists on the electric system reliability, resource adequacy risks have received less attention. As part of a study into electricity reliability more broadly, (Hines et al., 2009) find that supply shortages over the period 1984–2006 were responsible only for 2.3% of U.S. outage events. The methods used by system planners today are very similar to those outlined by Billinton in the 1970s (Billinton et al., 1973). More recently, system planners have begun to analyze the economically optimal reserve margin, or the reserve margin that minimizes total system costs and outage costs (Pfeifenberger et al., 2013; Newell et al., 2014).

In this paper, we analyze the resource adequacy requirements of the PJM Interconnection. We evaluate the sensitivity of requirements to the choice of metric used to measure resource adequacy: LOLE, LOLH, and Unserved Energy. Because the choice of reliability metric is somewhat arbitrary, it would behoove system operators in PJM and elsewhere to understand how capacity procurements may change under different resource adequacy metrics. We also evaluate the reserve margin that results in the lowest long-run system costs, known as the economically optimal reserve margin. We develop a robust statistical model of resource adequacy in PJM for the year 2010. The model consists of a probabilistic forecast of hourly load and a probabilistic forecast of generator outages. The load model explicitly considers three major drivers of uncertainty: uncertain load growth, natural temperature variability, and uncertainty in the underlying model/process. The load model uses ten years of load data and sixty years of temperature data from Pittsburgh International Airport and Reagan National Airport. We combine the load and outage models into a probabilistic forecast of supply shortages. The model is structurally similar to the model used by PJM to forecast load. The intent of this model is not to improve upon PJM's load forecasting methods. Rather, the intent is to allow us to explore the sensitivity of PJM's load procurement decisions to factors including the choice of reliability metric, how likely they wish to meet the target, and risk of correlated failures among generators.

In 2010, PJM calculated a 15.5% reserve margin was needed to achieve the 0.1 LOLE standard. PJM procured additional capacity, making the realized reserve margin 20.5%. We find that PJM's 15.5% reserve margin target met the 0.1 LOLE standard. By procuring additional capacity such that the actual reserve margin was 20.5%, PJM's realized LOLE was 0.012 events per year, and PJM met the 0.1 LOLE standard with 90% confidence. Switching to the 2.4 LOLH or 0.001% UE standard would allow PJM to reduce reserve margins to 13% and maintain current risk preferences. This represents an 11 GW reduction in capacity from a 20.5% reserve margin. PJM anticipates 11 GW of coal capacity, or ~7% of total capacity, is "at high risk" of retirement (PJM, 2011b). We find that this 11 GW of high risk coal capacity could retire if PJM were to switch to the LOLH or UE metric. We also find that the economically optimal reserve margin in PJM was 13–15%, which would minimize long-run total system costs, including costs for energy, capacity, reserve shortages, and outages.

An emerging source of risk in power systems is the risk of multiple generators failing simultaneously due to an external forcing event. Traditional system planning assumes plant fail independently of one another. The risk of correlated generator failures was exposed in January 2014, when extreme cold temperatures in the Northeast and Mid-Atlantic forced many generators offline simultaneously due to fuel shortages and mechanical failures and threatened reliability (PJM, 2014c). PJM and other systems are working to reduce the risks posed by winter fuel supply disruptions. However, other types of correlated failure risks exist, including extreme weather and natural disasters. Unfortunately, quantifying the likelihood and magnitude of such correlated failures is difficult due to their infrequency.

We illustrate the potential risks posed by three types of correlated failures: (1) natural gas supply disruptions that force all gas generators offline, (2) increased outage rates among all plants during winter months due to mechanical and fuel supply issues, and (3) the forced shutdown of all PJM nuclear generators by regulators, such as happened in Japan post-Fukushima. We do not attempt to quantify how likely such correlated failures may be. Rather, we vary the likelihood of correlated failures occurring and see the effect on reliability. We find that such low probability but high impact correlated failures may have a large effect on reliability, and may cause PJM and other system operators to overstate reliability.

We also find that the distribution of outage size is 'fat tailed', and the largest 10% of outages account for half of total load shed. Therefore, system operators should recognize that supply shortages are more rare, but more disruptive than implied by reliability metrics.

2. Methods

We develop a probabilistic forecast of supply shortages in PJM for 2010. This forecast consists of two separate analyses: a probabilistic simulation of hourly load, and a probabilistic simulation of capacity available at each hour. These analyses are described in detail below. We then use Monte Carlo analysis to find the probability that load exceeds supply for each hour of the year. We analyze three reliability metrics: LOLE, LOLH, and UE, and their sensitivity to PJM's reserve margin. We perform several sensitivity analyses, and compare the results of our simulation to PJM's modeling of capacity needs.

2.1. Load forecast

We use historic load and temperature data to forecast load in

PJM. Load forecasts have three sources of uncertainty: uncertainty in load growth, natural temperature variability, and uncertainty in the underlying model/process. We consider each separately to robustly forecast load.

A large literature exists on forecasting load. Techniques commonly used include regression analysis, time-series analysis, and neural networks (PJM, 2013; Hagan and Behr, 1987; Hippert et al., 2001). The model used by PJM to set reserve margin targets is a probabilistic model derived from Billinton (PJM, 2003; Billinton et al., 1973). The model is not regression based, but uses heuristics that PJM has developed over time. PJM uses a separate regression model to forecast long-term load growth (PJM Interconnection, 2013).

We use regression analysis to forecast hourly load in PJM. The regression model shares many features in common with the regression model PJM uses to forecast long-term load growth. Regression analysis is useful for estimating the expected value of load at each time period. However, our focus is extreme events, i.e. high-load hours in which outages are more likely. To account for these extreme events, we bootstrap the model's residuals to simulate uncertainty in load at each time period.

We forecast hourly load in 2010 using hourly data from the previous ten years. Using ten years of load data allows us to develop a robust relationship between load and other explanatory variables. Hourly load data are from PJM (2014a). Hourly temperature and associated weather data is from the National Oceanic and Atmospheric Association (NOAA) for the Reagan National Airport and Pittsburgh International Airport weather stations (NOAA, 2014a). These weather stations were chosen as they have reliable temperature data available dating back to the 1940s, which is used to forecast 2010 temperatures. Data on the minutes of daylight for each day is from (US Naval Observatory, 2012) for Washington DC.

Since its inception, the PJM territory has undergone several expansions (Table 1). To account for these expansions, we forecast load separately for "PJM Classic" (the PJM region prior to any expansions) and each expansion zone. We then combine the forecasts into an overall PJM load forecast.

For each zone, the analysis has the following seven steps:

2.1.1. Step 1: regress long-term trend

We first identify and remove the ten year, long-term trend in load growth. By removing the long-term trend, we are able to explicitly incorporate PJM's forecast of future load growth (step 6). To remove the long-term trend, we use a non-parametric, additive model and regress load against the hour index, as shown in Eq. (1).[1] The hour index starts at 1 for the first hour of 2000, and ends at the last hour of 2009. Using an additive model allows us to account for nonlinearities in load growth, and regressing the logarithm of load allows us to account for higher variability at high-load hours. The model's residuals are stationary. We use these residuals in step 2 to control for additional explanatory variables that can cause load to vary throughout the year, including temperature and holidays. Fig. 1 shows the long-term trend of "PJM Classic", the original PJM footprint, and the model's stationary residuals.

$$\log(load_t) = f(t) + \beta_t \quad (1)$$

Table 1
PJM Expansions, 1993–2010 (PJM, 2014a).

Expansion	Date
Rockland Energy	March 2002
Allegheny Energy	April 2002
Exelon – Commonwealth Edison	May 2004
AEP	October 2004
Dayton Power & Light	October 2004
Duquesne Light Co	January 2005
Dominion Virginia	May 2005

2.1.2. Step 2: regress stationary time series

The second step is to regress β_t, the stationary residuals from step 1, on explanatory variables, including calendar events such as major holidays and weekends, temperature, and length of daylight hours. This is shown in Eq. (2). For hour of the day and length of daylight hours, we include interaction terms with the month of the year to account for changes in electric load patterns throughout the year. Table A.2 lists all explanatory variables. We use model's residuals, γ_t to account for uncertainty in the underlying model/process (see step 7).

$$\beta_t = \gamma_1 weekday + \gamma_2(hour{*}month) + \gamma_3 holidays + \gamma_4 Tadj, av\ g_D + \gamma_5(daylightHours{*}month) + \gamma_t \quad (2)$$

We use hourly weather data to calculate the $Tadj,avg_D$, the average daily temperature adjusted for wind chill index (WCI) and temperature humidity index (THI) (Table 3, Eqs. (3)–(6)). For each region, we use data for either Reagan National Airport (DCA) or Pittsburgh International Airport (PIT) (NOAA, 2014a), depending on which is closest (Table 2).

Because the relationship between temperature and load is highly nonlinear (Fig. 2), we used a nonlinear, additive term to account for temperature in the regression. The remaining regression terms are linear. We found that using a non-linear model of temperature was more accurate than a linear model of temperature dependence that included both linear and quadratic terms (see Appendix A). As shown in Figs. A.2–A.4, the linear model significantly over-predicts load during high-temperature days. This is because the linear model predicts accelerating growth in load with increasing temperatures. However, load growth actually begins to slow once an average daily temperature of ~27 °C are reached (Fig. 2). This is likely because air conditioning loads start to saturate once temperatures are high enough. This over-prediction of peak load hours causes the linear model to overstate LOLE (Fig. A.5). Due to this bias in the linear model, we use a non-linear model in our main analysis.

2.1.3. Step 3: bootstrap residuals of the stationary model

To account for uncertainty in the underlying process/model, we bootstrap the residuals of the stationary time series model, γ_t , Eq. (2). We bootstrap residuals by month, in 24-h blocks. Bootstrapping by month allows us to account for heteroskedasticity in the residuals (Fig. A.6); using 24-h blocks allows us to account for time dependence in the residuals (Fig. A.7). The resulting bootstrapped residuals are used in step 7.

2.1.4. Step 4: forecast temperatures

Because the next year's temperatures are uncertain, we develop temperature forecasts for 2010 based on historic NOAA weather data dating back to 1949 for DCA and PIT airports (NOAA, 2014a) (years 1966–1972 were excluded due to missing data). We use hourly temperature, relative humidity, and wind speed data to calculate the average adjusted daily temperature ($Tadj,avg_D$) for DCA and PIT each day (Table 3, Eqs. (3)–(6)). We bootstrap days from this 60 year dataset, by month, in 10-day blocks. Bootstrapping by month allows us to account for the seasonal

[1] The non-parametric function $f(\cdot)$ is estimated using R software and *gam* command from "gam" package in R with default settings where splines are used for the non-parametric estimation (see (Hastie, 2013)).

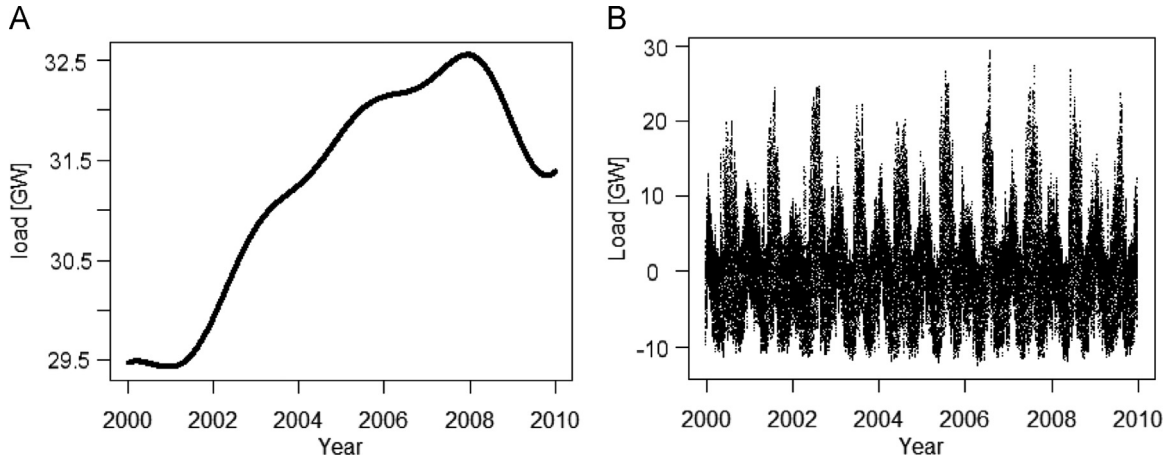


Fig. 1. (A) Fitted long-term trend and (B) stationary hourly residuals, β_t, for PJM Classic.

Table 2
Weather station used for each zone's regression.

Region	Weather station used
PJM Classic	DCA
Rockland Energy	DCA
Allegheny Energy	DCA
Exelon – Commonwealth Edison	PIT
AEP	PIT
Dayton Power & Light	PIT
Duquesne Light Co	PIT
Dominion Virginia	DCA

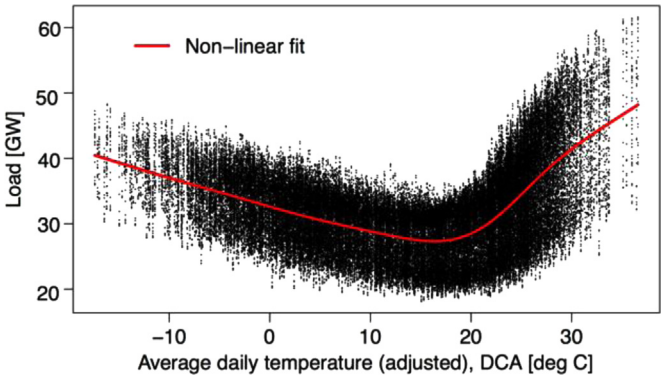


Fig. 2. Relationship between hourly load in PJM Classic and adjusted average daily temperature at Reagan National Airport (DCA), 2000–2009. Because the relationship is highly nonlinear, we use a non-linear, additive model to account for temperature dependence.

variations in temperature; using 10-day blocks allows us to account for time dependence in weather patterns that can last for several days (Fig. A.8). Using 60 years of temperature data allows us to robustly account for extreme temperatures that may occur. We do not observe a secular trend in the NOAA temperature data. By using historic data, we do not account for the possibility of future climate-induced changes in temperature levels or volatility.

2.1.5. Step 5: forecast the stationary time series

Once we have a model of the underlying stationary process (step 2), we use the model to predict the next year's stationary time series. This stationary time series excludes the effects of load growth. In this prediction, we use the temperature forecast developed in step 4.

Table 3
Temperature calculations.

$$THI_i = c_1 + c_2T_i + c_3R_i + c_4T_iR_i + c_5T_i^2 + c_6R_i^2 + c_7T_i^2R_i + c_8T_iR_i^2 + c_9T_i^2R_i^2 \quad (3)$$

$c_1 = -42.379$
$c_2 = 2.04091523$
$c_3 = 10.14333127$
$c_4 = -0.22475541$
$c_5 = -6.83783 \times 10^{-3}$
$c_6 = -5.481717 \times 10^{-2}$
$c_7 = 1.22874 \times 10^{-3}$
$c_8 = 8.5282 \times 10^{-4}$
$c_9 = -1.99 \times 10^{-6}$

$$WCI_i = 35.74 + 0.6215T_i - 35.75V_i^{0.16} + 0.4275TV_i^{0.16} \quad (4)$$

$$Tadj_i = \begin{cases} THI_i, & \text{if } T_i \geq 80^o F \text{ and } R_i \geq 40\% \\ WCI_i, & \text{if } T_i \leq 50\ ^o F \text{ and } V_i \geq 3 \text{ mph} \\ T_i, & \text{otherwise} \end{cases} \quad (5)$$

$$Tadj, avg_D = mean(Tadj_i), \forall\ i \in D \quad (6)$$

i = hour of the day
D = day of the year
T_i = hourly temperature [°F]
R_i = hourly relative humidity [percentage value between 0 and 100]
V_i = hourly wind speed [mph]
THI_i = temperature humidity index [°F]
WCI_i = wind chill index [°F]
$Tadj_i$ = hourly adjusted temperature
$Tadj,avg_D$ = daily average adjusted temperature [°F]
WCI index equation from (NOAA, 2013); THI index equation based on (NOAA, 2014b).
Although conversion equations are in English units, the remainder of our analysis uses Celsius.

2.1.6. Step 6: forecast load growth

Our forecast of growth in average load is based on PJM's 2009 forecast for 2010 load growth. We adjust the forecast to account for the historic accuracy of the Energy Information Agency's (EIA) load forecasts in the Annual Energy Outlook; insufficient data on PJM forecast accuracy is publically available. Between 1999 and 2008, EIA load growth forecasts had an average bias of −0.3% and

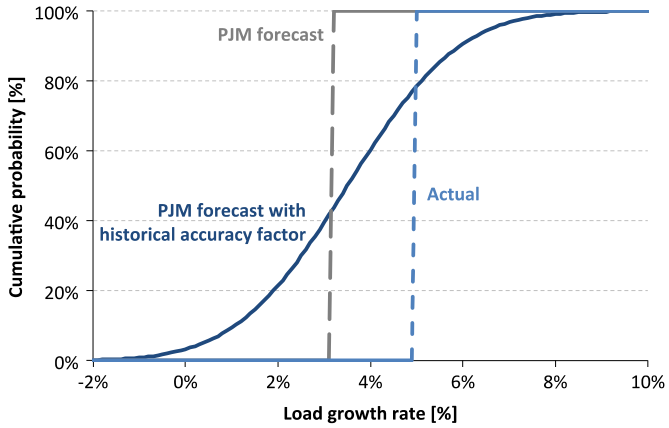


Fig. 3. PJM's 2010 load growth forecast, with and without the historical accuracy factor, and actual load growth that occurred.

standard deviation of 1.9% (EIA, 2008). We assume forecast errors are normally distributed, and develop a distribution of possible load growth rates (Fig. 3). We then sample growth rates from the resulting distribution. We assume load growth is linear throughout the year.

2.1.7. Step 7: forecast hourly load

Finally, we sum the three components of our load forecast model: forecast load growth (step 6), the forecast stationary time series (step 5), and the residuals of the stationary time series regression (step 3). This allows us to separately account for the three sources of uncertainty: uncertain load growth, natural temperature variability, and uncertainty in the underlying model/process. As all three components are probabilistic, we repeat the process many times to measure the uncertainty associated with each. The result is a probabilistic hourly forecast of load.

Once we have developed probabilistic hourly load forecasts for each zone, we sum these forecasts to find the total load forecast for PJM. We repeat the entire process 5000 times to develop a probabilistic forecast of hourly PJM load in 2010.

2.2. Supply forecast

We next forecast the total capacity available at each hour. Total available capacity is the summed capacity of all online dispatchable plants, demand response, import capacity, and firm wind capacity. We use data from the 2010 PJM Form EIA-411 to identify each dispatchable plant's summer and winter capacity, as cleared in the capacity auction (PJM, 2010b). We therefore assume the system operator has perfect information as to what generators will be available for the forecast year. We simulate the online status of each PJM generator, taking into consideration forced outages, planned outages, and maintenance outages. We simulate total capacity available for each of the 8760 h of the year, and repeat the simulation 5000 times to get a distribution of capacity available at each hour. We do not model other supply-side actions PJM can take to mitigate outage risks, such as voltage reductions.

We first schedule planned outages and maintenance outages for all plants. These outages are scheduled such that the likelihood of a supply shortage is minimized. As such, the majority of outages are scheduled during the spring and fall. NERC's Generating Availability Data System (GADS) provides data on the average number of planned outage hours and maintenance outage hours for plants, aggregated by plant type and size (NERC, 2014). We find that these outages can be scheduled with minimal effect on LOLE. We schedule each plant's planned outages and maintenance outages with the following process:

1. Find the total planned outage hours (POH) and forced outage hours (FOH) for each plant.
2. Divide plants into two categories: peaking plants and non-peaking plants. We identify peaking generators as natural gas combustion turbines smaller than 100 MW and oil generators.
3. Schedule peaking outages such that the total offline capacity is roughly equal for all hours of the year. Each plant is assumed to undergo one outage, of duration POH+FOH. ~1.7 GW of peaking capacity is scheduled offline each hour.
4. Schedule non-peaking outages to occur during the spring (March–May) and fall (September–November). Each plant is assumed to undergo one outage, of duration POH+FOH. ~35 GW of non-peaking capacity is scheduled offline each spring and fall hour.

By scheduling outages in this manner, we minimize the likelihood of a supply shortage. We also mimic the actual scheduling of outages in PJM, in which baseload coal and combined cycle plants are primarily offline during the spring and fall, and combustion turbines are offline throughout the year (Fig. A.1).

We next model forced outages. Forced outages are caused by unforeseen technical problems, occur randomly throughout the year, and have an uncertain duration. We model plant forced outages as a two-stage discrete Markov chain (Billinton et al., 1973). Fig. 4 illustrates this process. At each time period t, if the plant is online there is probability $P_{1,1}$ that it remains on at period $t+1$ and probability $P_{1,0}$ that is fails. If the plant is offline, it remains off with probability $P_{0,0}$ and is repaired with probability $P_{0,1}$. Accounting for the duration of outages increases the uncertainty of how much capacity is available at each hour. We simulate each plant's forced outages over one year (8760 h), then sum the total online capacity of all PJM plants. We assume that each plant's transition probabilities are constant throughout the year.

GADS provides data on the mean number of forced outages, and PJM provides data on plant equivalent demand forced outage rates (EFORd) (PJM, 2014b). We use these data to calculate the transition probabilities with Eq. (7) through (11) (Table 4). EFORd is defined as "the probability that a generating unit will fail, either partially or totally, to perform when it is needed to operate" (PJM, 2011a). All data are aggregated by plant type and size.

We estimate the available DR capacity and net import capacity based on the results of the capacity auctions (PJM, 2009) (Table 5). Each auction covers the period of June 1 of the first year to May 31 of the second year. We derate DR capacity by 5%, as is PJM's practice to account for DR that does not respond to PJM requests (PJM, 2010a). Firm wind capacity is assumed by PJM to be 13% of nameplate capacity (PJM, 2009); for both 2009 and 2010, firm wind capacity was 40 MW.

2.3. Outage forecast

We assume here that an outage occurs when total load exceeds total available capacity. Using the procedures outlined above, we develop yearly forecasts of hourly load and available capacity. We then subtract the hourly load forecast from the hourly forecast of available capacity to identify if an outage has occurred, Eq. (12)

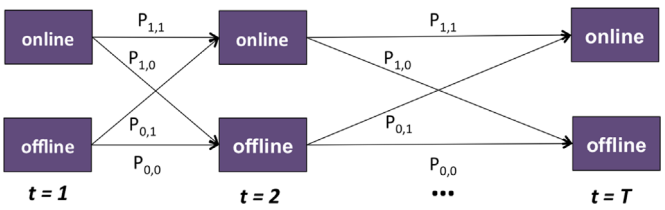


Fig. 4. Forced outages 2-stage discrete Markov process.

Table 4
Forced outage equations.

$$MOD = \frac{EFORd*8760}{NFO} \quad (7)$$

$$P_{0,1} = \frac{1}{MOD} \quad (8)$$

$$P_{0,0} = 1 - P_{0,1} \quad (9)$$

$$P_{1,0} = \frac{NFO}{8760} \quad (10)$$

$$P_{1,1} = 1 - P_{1,0} \quad (11)$$

MOD=mean outage duration
NFO=Annual number of forced outages
$EFORd$=Equivalent forced outage rate

Table 5
DR capacity and net import capacity, by capacity auction (PJM, 2009).

Capacity auction	DR capacity (MW)	Net import capacity (MW)
2009/2010	7290	+320
2010/2011	9050	−400

Table 6
Outage equations.

$$Outage_i = \begin{cases} 1 : \sum AvailableCapacity_i < Load_i \\ 0 : \sum AvailableCapacity_i > Load_i \end{cases}, \forall i \in I \quad (12)$$

$$LOLH = \sum_i Outage_i, \forall i \in I \quad (13)$$

$$EUE = \sum_i (Load_i - AvailableCapacity_i), \forall i \in Outage_i = 1 \quad (14)$$

I=set of 8760 annual hours
AvailableCapacity i =summed capacity of all online PJM generators, DR, net imports, and reliable wind power at hour *i*
Load i=total PJM load at hour *i*
Outage i=binary variable indicating if an outage occurred at hour *i*

(Table 6). We calculate UE and LOLH with Eqs. (13) and (14) to find the number of outages per ten simulated years (Table 6). LOLE is calculated in a similar manner as LOLH, but all consecutive outage hours are counted as one outage event. We repeat the process 10,000 times to develop distributions of LOLE, UE, and LOLH. We repeat the entire process, varying the amount of installed capacity in order to see how reliability metrics change versus reserve margin. To vary capacity, we add or subtract a constant amount from each hour's available capacity.

Our modeling does not consider the effect of transmission constraints on resource adequacy. In the 2009/2010 auction, PJM found inflows were constrained to the Eastern Mid-Atlantic Area Council (EMAAC) and southwestern MAAC. Additional capacity was procured in these regions, resulting in higher capacity prices in these regions (PJM, 2008). In the 2010/2011 auction, PJM found no transmission constraints, and capacity prices were equal throughout the interconnection. We also ignore any operating or synchronous reserve requirements.

PJM's Base Residual Auction is held in May, three years prior to the delivery year. By conducting the auction three years in advance, PJM seeks to reduce uncertainty for market participants. Each year after the Base Residual Auction, PJM conducts Incremental Auctions to account for changes in market conditions. Our analysis simulates the last Incremental Auction, one year in advance of the delivery date. As such, we use data from 2009 and earlier to develop the 2010 forecast. In principle, our methods could be used to simulate the Base Residual Auction, but would need to be adjusted to account for the increased uncertainty in available capacity and load three years in advance.

2.4. Economically optimal reserve margin

We analyze the level of capacity procurement that minimizes long-run total system costs. We use PJM generator data and load data from 2010 in this analysis. We consider costs from four sources: costs on the capacity market, energy market, outage costs, and reserve shortage costs. In 2010, PJM's reserve margin (installed capacity) was 20.5%. We quantify total system costs for reserve margins of 10–20%. These methods are similar to those used by other studies of the economically optimal reserve margin (Newell et al., 2014; Pfeifenberger et al., 2013).

The consequences of reducing PJM's reserve margin depend greatly on the type of capacity that is no longer procured (retired). Procuring less capacity would force the retirement of plants with the highest capacity market bids. However, individual capacity market bids are not publically available, and therefore we cannot know which plants would retire. If baseload capacity retired, costs on the energy market increase significantly. If peaking capacity retired, energy market costs would be unchanged.

We assume procuring less capacity would force the retirement of coal plants that are expensive to operate. PJM has identified 11 GW of coal capacity “at high risk” of retirement, and an additional 14 GW of coal capacity “at some risk” of retirement (PJM, 2011b). These plants are smaller than 400 MW and older than 40 years. However, it is possible that lower reserve margins might force other types of capacity to retire. We therefore bound our analysis with two scenarios: only baseload plants retire, and only peaking plants retire.

We evaluate four types of system costs: costs on the capacity market, energy market, outage costs, and reserve shortage costs. Total system costs are approximated as the sum of these four cost categories. We exclude several other types of costs, including costs on regulation markets, emergency import costs, and demand response costs. Although these categories are small relative to the costs considered here (Newell et al., 2014), future work could consider these and other system costs.

We quantify energy market costs with a reduced form supply curve dispatch model. Energy market costs are calculated as the sum of generator fuel and variable operation and maintenance costs throughout the year. We assume generators are dispatched each hour in order of least cost. We do not capture constraints that can lead to out-of-merit-order dispatch, such as transmission constraints and generator ramping constraints. We use 2010 hourly load data and generator capacity data from PJM (2010a,

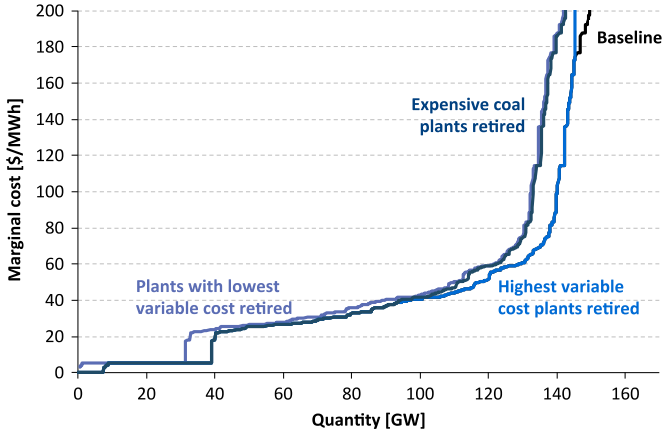


Fig. 5. Energy market supply curves for baseline 20.5% reserve margin, and 15.5% reserve margin with different types of capacity retired.

2010b) to estimate energy costs. We derate each plant's capacity by the forced outage rate (PJM, 2011a). Delivered fuel cost data is from EIA (2014b) and Lazard (2010). Variable operation and maintenance costs are from Lazard (2010). Plant heat rates are from eGRID (EPA, 2014). As shown in Fig. 5, the baseline scenario retires the most expensive coal plants to operate. For the sensitivity analysis, we retire plants with the lowest operating costs (baseload) and highest operating costs (peakers).

We estimate long run capacity costs as the total cost of building and operating a new natural gas combustion turbine (NGCT) plant, net expected revenues on the energy market (net CONE). We approximate this quantity, known as the net cost of new entry (net CONE), as $100/kW-yr based on findings of existing studies (Spees et al., 2011).

We assume a reserve shortage occurs in any hour of the year H when hourly load is high enough to force PJM to draw from their day ahead schedule reserves (DASR) (Eq. (15)). Shortages are valued at PJM's current price cap of $2,700/MWh (PJM, 2014e). Hourly 2010 DASR data is from PJM (2014f).

$$ReserveShortage_h = \min(0, Load_h - (totalCapacity - ReserveRequirement_h)), \forall h \in H \quad (15)$$

The cost of an outage is the total unserved energy (UE), multiplied by the value of lost load (VoLL) of consumers. We multiply the simulated UE values by an assumed VoLL to approximate the total cost of outages. We assume a VoLL of $15/kWh, based on the estimated costs of a one hour interruption for medium/large commercial and industrial consumers (Sullivan, 2009).

2.5. Correlated outages

Next, we evaluate the risk posed by low probability but high impact events that can force the correlated failure of multiple generators simultaneously. Traditional resource adequacy planning does not account for such risks. We do not attempt to quantify the probability of such correlated failures occurring. Rather, we vary the likelihood of correlated failures and test how resource adequacy metrics change.

First we test how LOLE, LOLH, and UE would vary if all 50 GW of PJM natural gas generators were subject to the risk of a natural gas supply disruption. We test the risk posed by supply disruptions that could occur at any point during the year, and we test the risk for supply disruptions that only occur during winter months

Table 7
Correlated outage equations.

$$fuelShortage_i = \begin{cases} 1: rand() \le P_{FS} \\ 0: rand() \ge P_{FS} \end{cases}, \forall i \in I_{winter} \quad (16)$$

$$P'_{1,0,i} = \begin{cases} P_{outage,FS}: fuelShortage_i = 1 \\ P_{1,0} - P_{outage,FS} * P_{FS}: fuelShortage_i = 0 \end{cases}, \forall i \in I_{annual} \quad (17)$$

$$P'_{1,1} = 1 - P'_{1,0} \quad (18)$$

I_{annual} = set of all 8760 annual hours
I_{winter} = set of 2160 winter hours
P_{FS} = Probability of a fuel shortage
$fuel\ Shortage_i$ = binary variable indicating if there is a fuel shortage at hour i
$P_{outage,FS}$ = Probability that a generator goes offline if a fuel shortage occurs

(December–February). We model the hourly risk of a fuel supply shortage as P_{FS}. We then evaluate each winter hour if a supply shortage occurs with Eq. (16) (Table 7). We assume the risk of a supply shortage is uniform throughout the winter. If a supply shortage occurs, the probability of each individual generator failing is $P_{outage,FS}$, Eq. (17) (Table 7); if no supply shortage occurs, we adjust the probability of an independent failure occurring such that the overall risk of failure is equal to the case in which all outages are independent, Eq. (10). We therefore do not change the probability of an outage occurring. Rather, we adjust the fraction of outages due to a supply shortage versus an independent failure. Because data on the frequency and severity of correlated outages is not publically available, we test the sensitivity to each parameter. First, we vary the hourly probability of a supply shortage such that the likelihood of a disruption occurring varies from twice per year/winter to once every 5 years/winters, assuming that all gas generators fail if a shortage occurs ($P_{outage,FS}=1$).

Second, we test how seasonal variations in plant reliability may affect resource adequacy. As evidenced by the 2014 Polar Vortex, extreme cold can cause outages at all types of generators. Coal, gas, and nuclear plants were all offline during the Polar Vortex due to reasons including mechanical failures, frozen pipes, frozen coal piles, and gas supply disruptions (PJM, 2014c). We test how system reliability change would change if plant EFORd were modeled as sensitive to ambient temperature. We model all plants as 50% less likely than baseline to be forced offline during the warmest 6 months (April–September) and 50% more likely to be forced offline in the coolest 6 months (October–March).

Third, we test the risk posed by all PJM nuclear generators shutting down simultaneously, as occurred in Japan due to regulatory intervention after the Fukushima Daiichi disaster. We assume the risk of such a correlated failures is constant throughout the year, and vary the likelihood of such an event occurring from once every 10 years to once every 50 years. We assume that such a regulatory intervention would force generators to be offline for an average duration of six months ($P_{01}=1/4330$, $P_{00}=1-1/4330$).

3. Results

Table A.1 shows accuracy statistics of the load model, both in the training data for 2000–2009 and test data when predicting 2010 load. The test error is the model's prediction error when given actual 2010 temperatures and load growth; it therefore

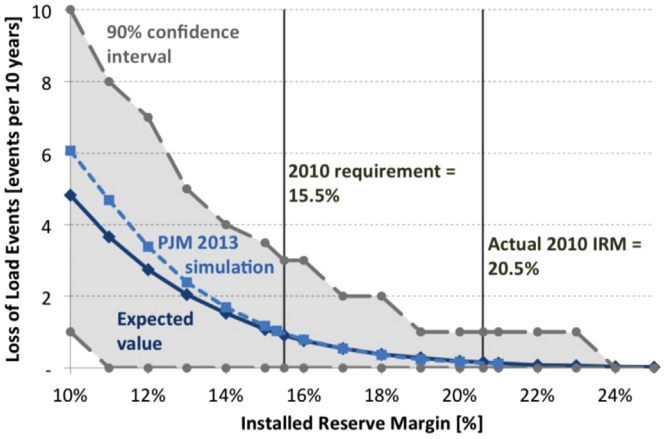


Fig. 6. 2010 LOLE versus reserve margin. Also shown are results from PJM's 2013 resource adequacy modeling (recreated from (PJM, 2010a)).

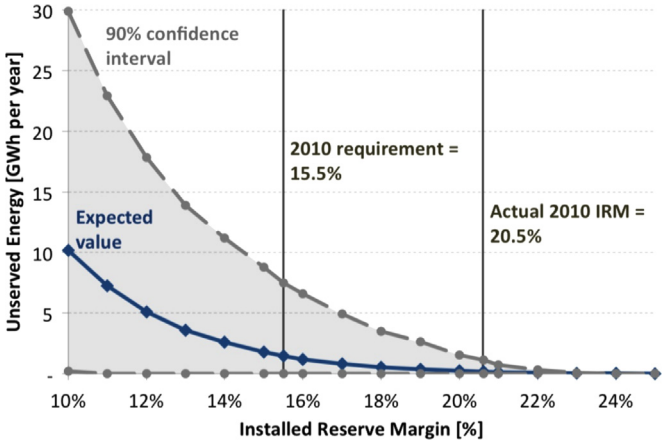


Fig. 7. 2010 unserved energy versus reserve margin.

ignores uncertainty in temperature and load growth. Normalized root-mean-square error (NRMSE) controls for the size of the PJM region, Eq. (19). Table A.2 shows detailed regression results for the "PJM Classic" region.

$$NRMSE = \frac{RMSE}{load_{max} - load_{min}} \quad (19)$$

The model's accuracy could certainly be improved further. Including weather data from more points within PJM would likely have the greatest effect on model accuracy. Our model uses weather data from Reagan National and Pittsburgh International Airports; PJM's long-term load forecasting model uses temperature data from 24 airports (PJM, 2013).

3.1. Reliability metrics

Fig. 6 shows simulated 2010 LOLE for reserve margins of 10–25%. The expected value of our 2010 simulation closely matches that of PJM's 2013 simulation (data on PJM's 2010 simulation is not available, but the results of the simulation have changed very little over time). In 2010, PJM found a 15.5% reserve margin was necessary to meet the 0.1 LOLE standard (PJM, 2010a); we find a 15.5% reserve margin would have resulted in an LOLE of 0.8 events per year. Our simulation's 90% confidence interval ranges from zero to three events per ten years at 15.5% reserve margin.

The actual 2010 reserve margin was 20.5% (164 GW), as PJM procured more capacity than was needed on the capacity market (PJM, 2008)[2]. We find that a 20.5% reserve margin corresponds to an expected LOLE of 0.012 events per year, and achieves the 0.1 LOLE standard with 90% confidence.

Fig. 7 shows simulated 2010 unserved energy versus reserve margin. At a 15.5% reserve margin, the expected UE is 1.1 GWh per year, or 0.00015% of actual 2010 load. The 90% confidence interval ranges from 0 GWh per year to 6.1 GWh per year (0.0000–0.0008% of load unserved, respectively). UE becomes increasingly uncertain at lower reserve margins. Expected LOLH is 3.4, with a 90% confidence range of 0–14.

We find that PJM's target 2010 reserve margin of 15.5% was sufficient to meet the 0.1 LOLE standard. Switching to either the 2.4 LOLH standard or the 0.001% UE standard could reduce reserve margins to 10% (Table 8). Procuring additional capacity such that the realized reserve margin was 20.5% implies PJM wishes to meet the 0.1 LOLE standard with 90% confidence. PJM could meet the 2.4 LOLH standard and 0.001% UE standard with 90% confidence at reserve margins of 13%. Requiring that the reliability metric be met with 95% or 99% confidence would further increase reserve margin requirements.

Table 8
Sensitivity of the target reserve margin and installed capacity to different reliability metrics and risk tolerances. PJM's target 2010 reserve margin was 15.5% (158 GW), and actual 2010 reserve margin was 20.5% (165 GW).

Metric	Optimal reserve margin [%] (installed capacity [GW])			
	Risk neutral	90% Confidence	95% Confidence	99% Confidence
0.1 LOLE	15.5% (158)	20.5% (165)	22% (168)	> 25% (> 170)
2.4 LOLH	10% (151)	13% (154)	14% (156)	15% (158)
0.001% UE	10% (151)	13% (154)	14% (156)	16% (159)

3.2. Economically optimal reserve margin

We estimate that PJM's long run, economically optimal reserve margin is 13–15%. System costs change by less than $100 million within this range, or less than 1% of the total $28 billion in estimated system costs. As shown in Fig. 8, costs associated with outages and reserve shortages become more significant as reserve margins fall below 14%. Above 14%, capacity market costs increase significantly. Because this range includes the 13% targets needed to meet the 2.4 LOLH standard and 0.001% UE standard with 90% confidence, we conclude that either of these standards could be

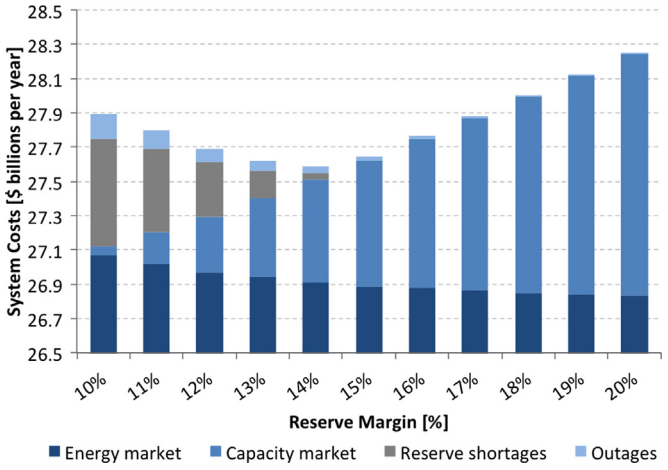


Fig. 8. Long run system costs. Capacity market costs above a $15 billion/year baseline.

[2] Generation offered + fixed resource requirement (FRR) commitments – generation offered but not accepted.

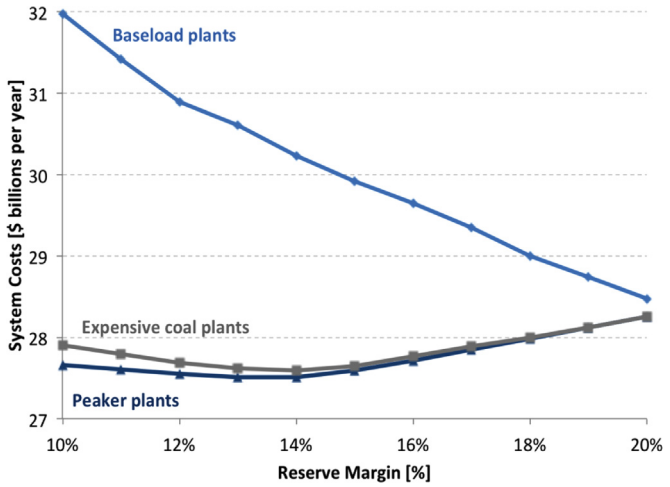


Fig. 9. Long run system costs, for different assumptions about what type of capacity is retired.

considered efficient. However, maintaining PJM's realized 2010 reserve margin of 20.5% would increase annual system costs by $600 million annually over a $15 billion per year baseline in the long run.

System costs are very sensitive to the type of capacity that is retired when PJM procures less capacity. As shown in Fig. 9, if the retired capacity is baseload plants, total system costs increase significantly as reserve margins decrease. If retired capacity are either expensive coal plants or peaker plants, system costs are minimized for reserve margins of 13–15%.

We find that outage costs are small in the long run, as the expected unserved energy is small. We therefore conclude that the economically optimal reserve margin is insensitive to VoLL, here assumed to be $15/kWh.

Our results are similar to those of other, similar studies (Newell et al., 2014; Pfeifenberger et al., 2013). Newell et al. found that the economically optimal reserve margin in the ERCOT system is 10.2%, lower than the reserve margin needed to meet the 0.1 LOLE standard. Similar to our results, the study found that system costs do not vary significantly for reserve margins of 8–14% but does note that there is more uncertainty in system costs at lower reserve margins. Consistent with these studies, we find that the economically optimal reserve margin in PJM is lower than the reserve margin needed to meet the 0.1 LOLE standard. Our results for PJM add to a growing body of literature suggesting that for a variety of systems the 0.1 LOLE may result in higher capacity procurements than are economically optimal in the long run.

3.3. Distribution of outage size

We find that there is extreme variation in the amount of load shed during outages. As shown in Fig. 10, the distribution of unserved energy resulting from an outage is extremely fat tailed. At a 15.5% reserve margin, the mean outage is 15 GWh, but outages range from 0 GWh to 110 GWh (Table 9). The top 10% largest outages account for half of total unserved energy, and the top 1% of outages account for 10% of total unserved energy. The risk of a very large outage becomes more pronounced at lower reserve margins.

3.4. Model form uncertainty

Load in PJM is highly sensitive to temperature, and accurately modeling this relationship is important for accurately calculating LOLE. We used a nonparametric, additive model to account for the relationship between load and temperature. We also tested a

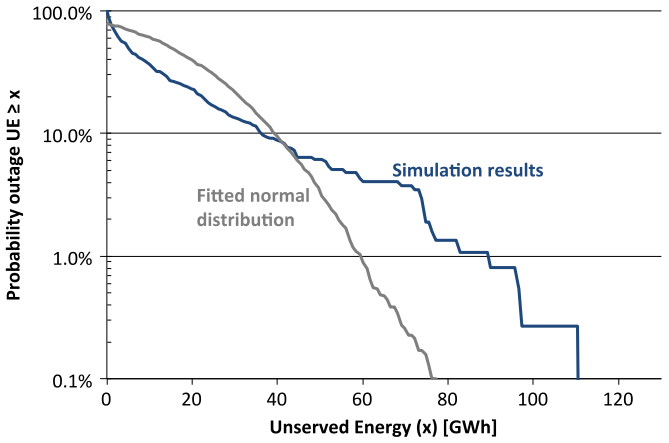


Fig. 10. Distribution of the size of simulated outages, in terms of unserved energy, versus a fitted normal distribution. Assumed reserve margin is 15.5%.

Table 9
Outage summary statistics, 15.5% reserve margin.

	Expected value	90% Confidence interval	Maximum
Outage duration [h]	4	1–9	10
Largest magnitude [GW]	3	0–10	17
Total load shed [GWh]	13	0–54	110

linear model to account for the relationship. The linear model divided days into heating degree days (HDD) and cooling degree days (CDD). Details can be found in Appendix A. We find that the linear model significantly over-predicts load at high temperature hours, which increases the modeled probability of outages relative to the nonparametric, additive model (Fig. A.5).

In our regressions, we hold each plant's forced outage rate (EFORd) constant throughout the year. Finally, we test the effects on LOLE of EFORd being sensitive to ambient temperature, with plants being 50% less likely to be forced offline during summer the warmest 6 months (April–September) and 50% more likely to be forced offline in the coolest 6 months (October–March).

3.5. Correlated failures

We find that natural gas supply disruptions have the potential to increase the risk of a supply shortage, assuming such outages

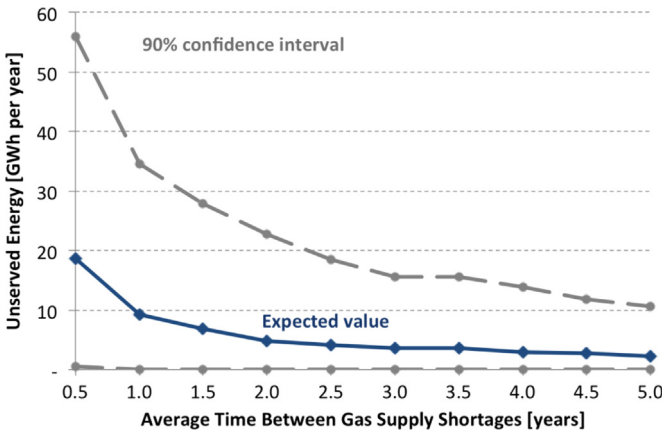


Fig. 11. Sensitivity of unserved energy to natural gas supply shortages that can occur at any point during the year, and force all PJM gas generators offline. Evaluated at 15.5% IRM.

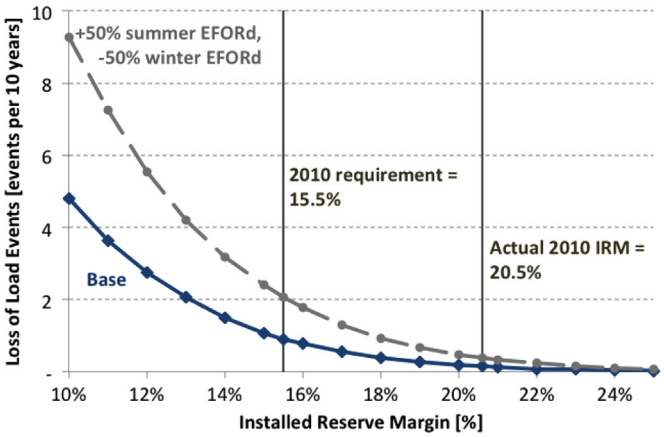


Fig. 12. Sensitivity of LOLE expected value to forced outage rate (EFORd).

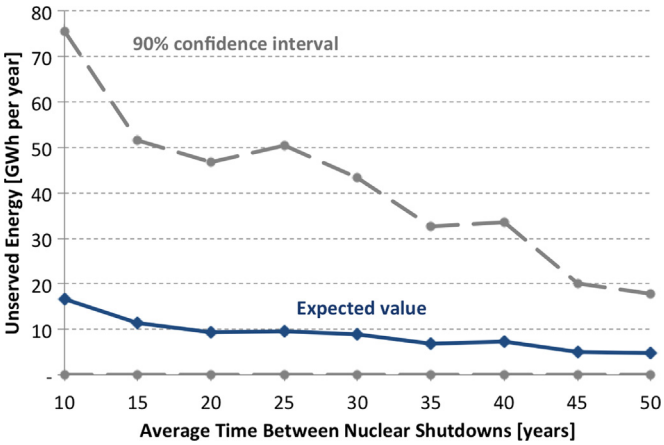


Fig. 13. Sensitivity of unserved energy to regulatory actions that force all PJM nuclear generators offline simultaneously for six months. Evaluated at 15.5% IRM.

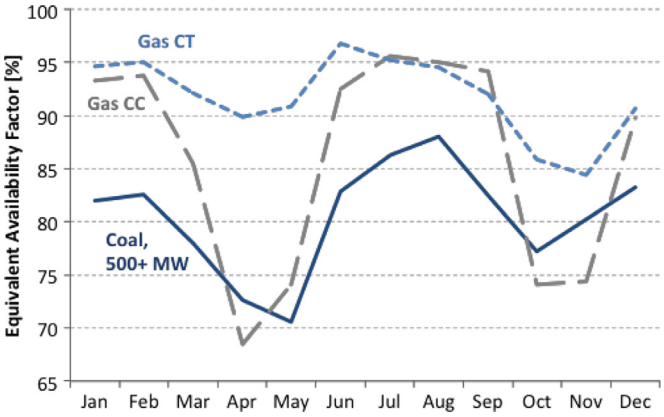


Fig. A.1. Equivalent availability factor, PJM generators, 2010 (Bresler, 2012).

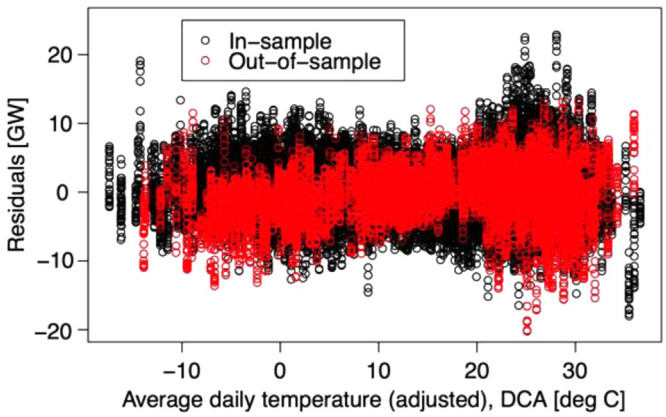


Fig. A.2. In-sample and out-of-sample residuals for PJM, linear model. Residuals are large at high temperature days.

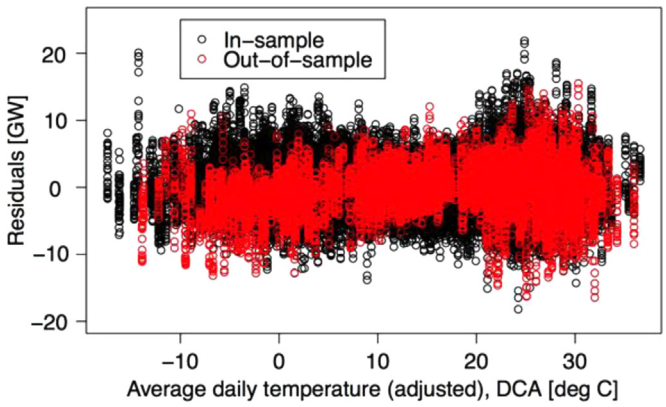


Fig. A.3. In-sample and out-of-sample residuals for PJM, non-linear model. The model is more accurate at predicting load during high temperature days than the linear model.

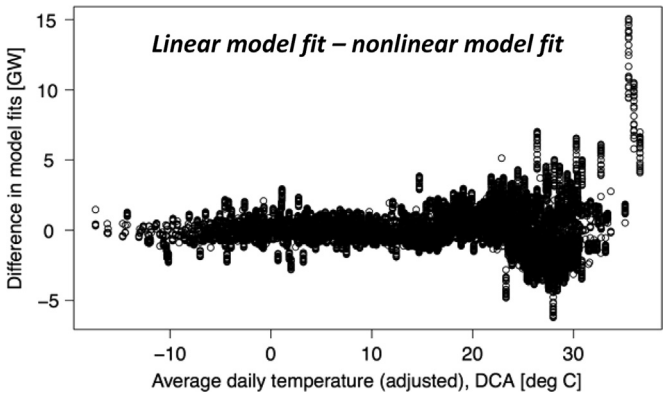


Fig. A.4. Difference in linear and nonlinear model fits, when predicting load out-of-sample.

force a large percentage of PJM's gas generators offline at once. If a supply disruption that forces all of PJM's gas generators offline were to occur on average once every fifth year, the expected UE would double (Fig. 11). Such supply disruptions can significantly increase the maximum size of supply shortages (Fig. A.9). Supply shortages that occur only during winter months do not have a significant effect on reliability.

We find that winter resource adequacy risks may be understated if plant reliability varies seasonally. If plant outage rates were 50% higher than baseline in winter months and 50% lower in summer months, system LOLE would more than double (Fig. 12).

However, our gas supply shortage analysis shows that winter gas supply disruptions alone do not significantly affect resource adequacy. As occurred during the 2014 Polar Vortex, mechanical and fuel supply issues at coal and nuclear generators during extremely cold days are also a significant contributor to winter resource adequacy issues.

We find that nuclear power supply disruptions also have the potential to increase the risk of a supply shortage. The likelihood of a regulatory action that forces all PJM nuclear generators offline simultaneously is unknown. However, we find that if such an action were to occur once every 50 years and force all nuclear

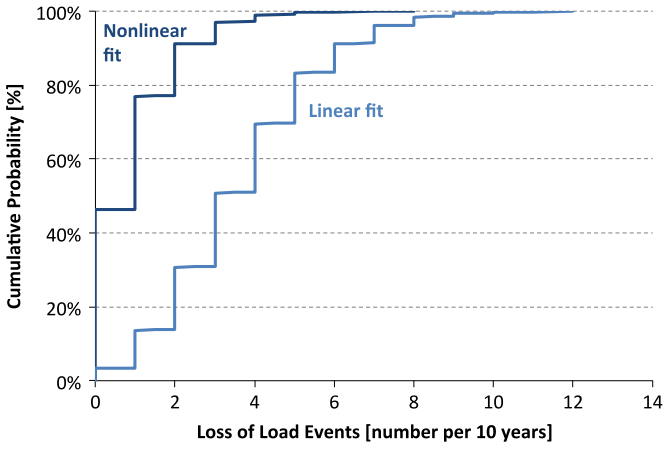


Fig. A.5. Calculated LOLE for linear and nonlinear models.

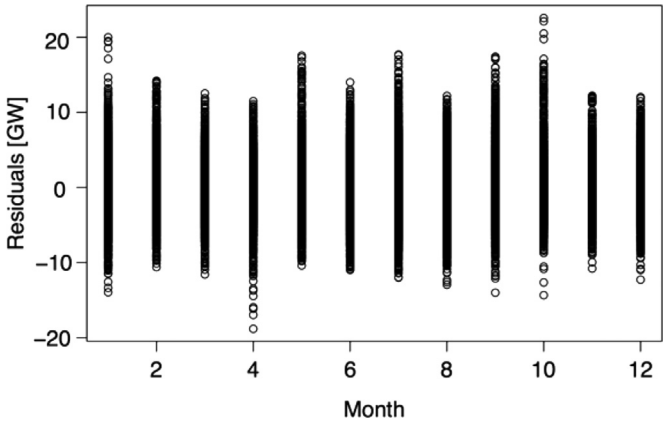


Fig. A.6. In-sample residuals, by month.

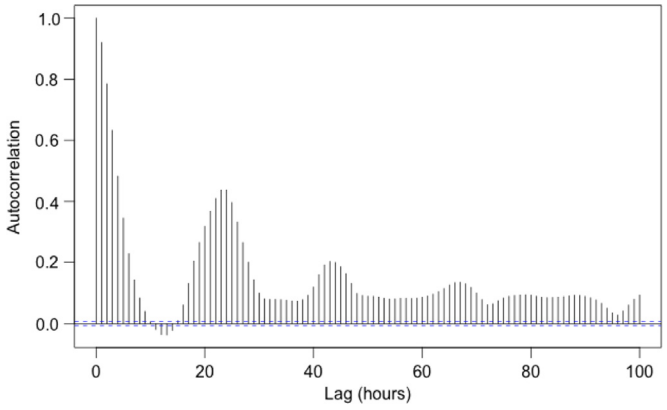


Fig. A.7. Autocorrelation of in-sample residuals.

generators offline for an average of 6 months, expected UE would quadruple (Fig. 13).

4. Discussion

Using our probabilistic regression method, we find the 2010 reserve margin target of 15.5% was sufficient to meet the mandated 0.1 LOLE standard. PJM procured 7 GW more capacity than needed to meet the 15.5% target, making the realized reserve margin 20.5%. By procuring more capacity than needed, PJM met the 0.1 LOLE standard with 90% confidence. This is due to PJM's policy to procure more capacity than needed if the capacity can be

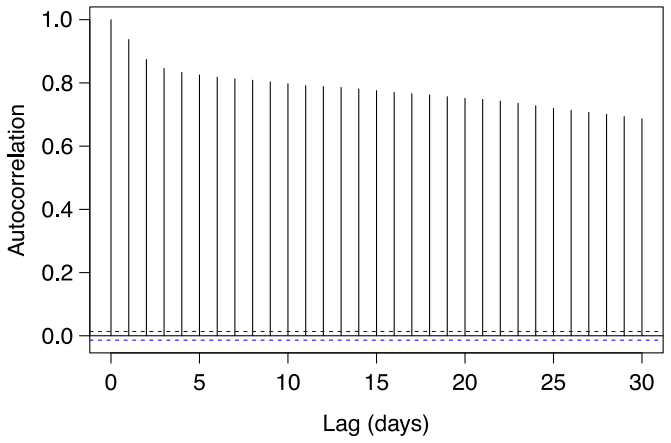


Fig. A.8. Autocorrelation function, average adjusted daily temperature. Data is for years 1949–2010, except 1966–1972.

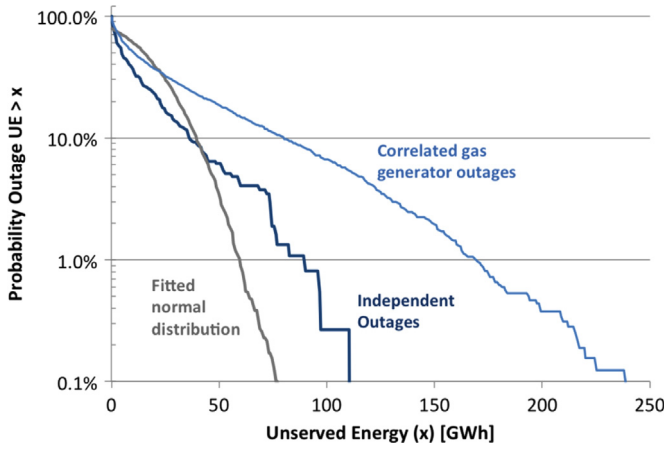


Fig. A.9. Distribution of outage size, in terms of unserved energy. Shown are both scenario in which outages are independent, and a scenario in which a natural gas supply shortage occurs on average once per year, forcing all gas generators offline at once. Assumed reserve margin is 15.5%.

Table A.1
Accuracy statistics of the load forecast model, both training error (2000–2009) and test prediction error (2010).

	Training, 1990–2009		Test, 2010	
PJM Region	**RMSE [MW]**	**NRMSE [%]**	**RMSE [MW]**	**NRMSE [%]**
PJM Classic	1690	4.0	1800	4.5
AEP	790	5.2	910	6.7
Allegheny Energy	300	5.3	330	6.2
Dayton Power & Light	130	4.7	140	6.1
Dominion Virginia	640	3.3	760	5.8
Duquesne Light Co	80	4.1	90	5.2
Exelon – Commonwealth Edison	930	5.6	1000	6.9
Rockland Energy	20	4.2	20	5.1
PJM total	3510	3.5	3840	4.3

procured at a cost less than the net cost of new entry of a natural gas combustion turbine (~$270/MW-day) (PJM, 2008; Spees et al., 2011).

Switching from the 0.1 LOLE standard to either the 2.4 LOLH or 0.001% UE standard would have reduced PJM's 20.5% reserve margin in 2010. A 13% reserve margin would have been sufficient to meet the 0.001% UE standard or the 2.4 LOLH standard with 90% confidence. This represents an 11 GW reduction in capacity

Table A.2
Detailed regression results for the PJM Classic region.

Variable	Estimate	Std. Error	*t* Value	Significance	Notes
(Intercept)	1.77E−01	2.81E−02	6.286	***	
isTue	1.07E−02	6.80E−04	15.694	***	
isWed	1.39E−02	6.81E−04	20.444	***	
isThu	1.46E−02	6.84E−04	21.289	***	
isFri	1.66E−03	6.89E−04	2.409	*	
isSat	−8.54E−02	6.83E−04	−125.053	***	
isSun	−1.15E−01	6.84E−04	−168.839	***	
isMLK	−1.08E−02	3.51E−03	−3.066	**	
isPresidentsDay	3.33E−03	3.54E−03	0.942		
isGoodFriday	−5.21E−02	3.49E−03	−14.962	***	
isMemorialDay	−1.01E−01	4.26E−03	−23.752	***	
isMemorialDayWeekend	−2.88E−02	2.71E−03	−10.602	***	
isJuly4	−1.14E−01	3.56E−03	−31.962	***	
isLaborDay	−1.13E−01	4.24E−03	−26.601	***	
isLaborDayWeekend	−2.28E−02	2.61E−03	−8.707	***	
isChristmas	−1.42E−01	4.63E−03	−30.571	***	
isXmasEveEve	−2.11E−03	4.63E−03	−0.456		Dec 23
isChristmasEve	−7.60E−02	4.63E−03	−16.405	***	Dec 24
isXMasWk	−2.53E−02	3.49E−03	−7.249	***	Dec 26–30
XMasLights	1.35E−02	2.64E−03	5.116	***	Dec 4– 22
isThanksgiving	−1.50E−01	3.78E−03	−39.591	***	
isThanksgivingFriday	−1.01E−01	3.78E−03	−26.69	***	Day after Thanksgiving
isNewYearsDay	−9.73E−02	3.60E−03	−27.021	***	
isNewYearsEve	−5.09E−02	4.53E−03	−11.234	***	
isThanksgivingWeek	−4.43E−03	1.94E−03	−2.28	*	Mon–Sun, Thanksgiving week
isXmasDayAfter	−4.67E−02	3.82E−03	−12.226	***	Dec 26
isFeb	5.69E−01	3.56E−02	15.97	***	
isH1	−1.27E−01	3.16E−03	−40.275	***	
isH2	−1.58E−01	3.16E−03	−49.848	***	
isH3	−1.71E−01	3.16E−03	−54.034	***	
isH4	−1.72E−01	3.16E−03	−54.256	***	
isH5	−1.52E−01	3.16E-03	−48.069	***	
isH6	−9.39E−02	3.16E−03	−29.672	***	
isH7	−2.94E−05	3.16E−03	−0.009		
isH8	5.38E−02	3.16E−03	16.991	***	
isH9	6.71E−02	3.16E−03	21.204	***	
isH10	7.29E−02	3.16E−03	23.044	***	
isH11	7.32E−02	3.16E−03	23.147	***	
isH12	6.47E−02	3.16E−03	20.432	***	
isH13	5.10E−02	3.16E−03	16.111	***	
isH14	3.91E−02	3.16E−03	12.351	***	
isH15	2.65E−02	3.16E−03	8.384	***	
isH16	2.57E−02	3.16E−03	8.106	***	
isH17	5.68E−02	3.16E−03	17.949	***	
isH18	1.31E-01	3.16E−03	41.321	***	
isH19	1.45E−01	3.16E−03	45.811	***	
isH20	1.32E−01	3.16E−03	41.601	***	
isH21	1.10E−01	3.16E−03	34.847	***	
isH22	6.87E−02	3.16E−03	21.71	***	
isH23	3.11E−03	3.16E−03	0.984		
isH24	−6.97E−02	3.16E−03	−22.036	***	
isMar	7.47E−01	3.43E−02	21.815	***	
isApr	6.20E−01	3.64E−02	17.054	***	
isMay	1.26E−02	4.36E−02	0.289		
isJun	−2.54E+00	1.17E−01	−21.658	***	
isJul	1.15E+00	6.10E−02	18.865	***	
isAug	7.86E−03	3.85E−02	0.204		
isSep	1.17E−02	3.62E−02	0.323		
isOct	3.58E−01	3.40E−02	10.54	***	
isNov	5.44E−01	3.85E−02	14.11	***	
isDec	1.59E+00	1.07E−01	14.806	***	
sun.hours	6.31E−04	4.97E−05	12.698	***	Daily daylight length, DC [mins]
isFeb:isH1	2.94E−02	4.52E−03	6.496	***	
isFeb:isH2	3.16E−02	4.52E−03	6.99	***	
isFeb:isH3	3.39E−02	4.52E−03	7.51	***	
isFeb:isH4	3.57E−02	4.52E−03	7.909	***	
isFeb:isH5	3.75E−02	4.52E−03	8.29	***	
isFeb:isH6	4.05E−02	4.52E−03	8.973	***	
isFeb:isH7	4.15E−02	4.52E−03	9.174	***	
isFeb:isH8	3.38E−02	4.52E−03	7.483	***	
isFeb:isH9	3.47E−02	4.52E−03	7.673	***	
isFeb:isH10	3.12E−02	4.52E-03	6.913	***	
isFeb:isH11	2.77E−02	4.52E−03	6.127	***	
isFeb:isH12	2.41E−02	4.52E−03	5.341	***	
isFeb:isH13	2.12E−02	4.52E−03	4.689	***	

Table A.2 (*continued*)

Variable	Estimate	Std. Error	*t* Value	Significance	Notes
isFeb:isH14	1.89E−02	4.52E−03	4.192	***	
isFeb:isH15	1.67E−02	4.52E−03	3.688	***	
isFeb:isH16	1.22E−02	4.52E−03	2.701	**	
isFeb:isH17	−1.83E−03	4.52E−03	−0.404		
isFeb:isH18	−2.08E−02	4.52E−03	−4.611	***	
isFeb:isH19	1.29E−02	4.52E−03	2.855	**	
isFeb:isH20	1.84E−02	4.52E−03	4.063	***	
isFeb:isH21	2.00E−02	4.52E−03	4.416	***	
isFeb:isH22	2.13E−02	4.52E−03	4.708	***	
isFeb:isH23	2.30E−02	4.52E−03	5.092	***	
isFeb:isH24	2.52E−02	4.52E−03	5.587	***	
isH1:isMar	2.87E−02	4.40E−03	6.519	***	
isH2:isMar	2.72E−02	4.40E-03	6.178	***	
isH3:isMar	2.67E−02	4.41E−03	6.059	***	
isH4:isMar	2.72E−02	4.40E−03	6.195	***	
isH5:isMar	2.92E−02	4.40E−03	6.644	***	
isH6:isMar	3.71E−02	4.40E−03	8.44	***	
isH7:isMar	3.88E−02	4.40E-03	8.829	***	
isH8:isMar	4.11E−02	4.40E−03	9.36	***	
isH9:isMar	4.70E−02	4.40E−03	10.692	***	
isH10:isMar	4.78E−02	4.40E−03	10.868	***	
isH11:isMar	4.79E−02	4.40E−03	10.889	***	
isH12:isMar	4.72E−02	4.40E−03	10.747	***	
isH13:isMar	4.69E−02	4.40E−03	10.665	***	
isH14:isMar	4.65E−02	4.40E−03	10.569	***	
isH15:isMar	4.39E−02	4.40E−03	9.977	***	
isH16:isMar	3.62E−02	4.40E−03	8.224	***	
isH17:isMar	1.16E−02	4.40E−03	2.641	**	
isH18:isMar	−3.90E−02	4.40E−03	−8.862	***	
isH19:isMar	−4.21E−03	4.40E−03	−0.957		
isH20:isMar	2.87E−02	4.40E−03	6.519	***	
isH21:isMar	3.69E−02	4.40E−03	8.388	***	
isH22:isMar	3.58E−02	4.40E−03	8.134	***	
isH23:isMar	3.14E−02	4.40E−03	7.15	***	
isH24:isMar	2.68E−02	4.40E−03	6.097	***	
isH1:isApr	1.18E−02	4.46E−03	2.636	**	
isH2:isApr	−7.41E−04	4.46E−03	−0.166		
isH3:isApr	−1.02E−02	4.49E−03	−2.278	*	
isH4:isApr	−1.43E−02	4.46E−03	−3.198	**	
isH5:isApr	−1.66E−02	4.46E-03	−3.731	***	
isH6:isApr	−9.39E−03	4.46E−03	−2.106	*	
isH7:isApr	−4.58E−03	4.46E−03	−1.026		
isH8:isApr	9.25E−03	4.46E−03	2.074	*	
isH9:isApr	3.23E−02	4.46E−03	7.236	***	
isH10:isApr	4.74E−02	4.46E−03	10.628	***	
isH11:isApr	6.00E−02	4.46E−03	13.452	***	
isH12:isApr	6.94E−02	4.46E−03	15.564	***	
isH13:isApr	7.70E−02	4.46E−03	17.276	***	
isH14:isApr	8.30E−02	4.46E−03	18.612	***	
isH15:isApr	8.46E−02	4.46E−03	18.97	***	
isH16:isApr	7.71E−02	4.46E−03	17.298	***	
isH17:isApr	4.44E−02	4.46E−03	9.96	***	
isH18:isApr	−2.94E−02	4.46E−03	−6.601	***	
isH19:isApr	−4.53E−02	4.46E−03	−10.158	***	
isH20:isApr	−1.10E−02	4.46E−03	−2.472	*	
isH21:isApr	4.67E−02	4.46E−03	10.472	***	
isH22:isApr	5.29E−02	4.46E−03	11.867	***	
isH23:isApr	4.13E−02	4.46E−03	9.253	***	
isH24:isApr	2.48E−02	4.46E−03	5.572	***	
isH1:isMay	−2.65E−02	4.54E−03	−5.847	***	
isH2:isMay	−4.77E−02	4.54E−03	−10.511	***	
isH3:isMay	−6.38E−02	4.54E−03	−14.05	***	
isH4:isMay	−7.67E−02	4.54E−03	−16.904	***	
isH5:isMay	−8.53E−02	4.54E−03	−18.801	***	
isH6:isMay	−8.81E−02	4.54E−03	−19.426	***	
isH7:isMay	−9.21E−02	4.54E−03	−20.297	***	
isH8:isMay	−6.09E−02	4.54E−03	−13.425	***	
isH9:isMay	−2.11E−02	4.54E−03	−4.655	***	
isH10:isMay	1.01E−02	4.54E−03	2.224	*	
isH11:isMay	3.70E−02	4.54E−03	8.158	***	
isH12:isMay	5.92E−02	4.54E−03	13.044	***	
isH13:isMay	7.75E−02	4.54E−03	17.077	***	
isH14:isMay	9.31E−02	4.54E−03	20.525	***	
isH15:isMay	1.04E−01	4.54E−03	22.816	***	
isH16:isMay	1.03E−01	4.54E−03	22.721	***	
isH17:isMay	7.34E−02	4.54E−03	16.182	***	

Table A.2 (*continued*)

Variable	Estimate	Std. Error	*t* Value	Significance	Notes
isH18:isMay	−4.80E−03	4.54E−03	−1.058		
isH19:isMay	−3.53E−02	4.54E−03	−7.788	***	
isH20:isMay	−3.07E−02	4.54E−03	−6.76	***	
isH21:isMay	1.94E−02	4.54E−03	4.281	***	
isH22:isMay	4.21E−02	4.54E−03	9.276	***	
isH23:isMay	2.59E−02	4.54E−03	5.702	***	
isH24:isMay	1.33E−03	4.54E−03	0.293		
isH1:isJun	−1.35E−01	6.43E−03	−20.974	***	
isH2:isJun	−1.65E−01	6.43E-03	−25.615	***	
isH3:isJun	−1.90E−01	6.43E−03	−29.586	***	
isH4:isJun	−2.12E−01	6.43E−03	−32.975	***	
isH5:isJun	−2.30E−01	6.43E−03	−35.685	***	
isH6:isJun	−2.51E−01	6.43E−03	−38.996	***	
isH7:isJun	−2.69E−01	6.43E−03	−41.868	***	
isH8:isJun	−2.30E−01	6.43E−03	−35.732	***	
isH9:isJun	−1.70E−01	6.43E−03	−26.446	***	
isH10:isJun	−1.20E−01	6.43E−03	−18.598	***	
isH11:isJun	−7.49E−02	6.43E−03	−11.645	***	
isH12:isJun	−3.60E−02	6.43E−03	−5.599	***	
isH13:isJun	−3.36E−03	6.43E−03	−0.523		
isH14:isJun	2.41E−02	6.43E−03	3.754	***	
isH15:isJun	4.57E−02	6.43E−03	7.101	***	
isH16:isJun	5.23E−02	6.43E−03	8.135	***	
isH17:isJun	2.46E−02	6.43E−03	3.832	***	
isH18:isJun	−5.61E−02	6.43E−03	−8.722	***	
isH19:isJun	−9.46E−02	6.43E−03	−14.705	***	
isH20:isJun	−1.09E−01	6.43E−03	−16.954	***	
isH21:isJun	−9.57E−02	6.43E−03	−14.886	***	
isH22:isJun	−6.48E−02	6.43E−03	−10.077	***	
isH23:isJun	−7.58E−02	6.43E−03	−11.785	***	
isH24:isJun	−1.00E−01	6.43E−03	−15.619	***	
isH1:isJul	3.20E−02	4.87E−03	6.575	***	
isH2:isJul	−2.08E−04	4.87E−03	−0.043		
isH3:isJul	−2.92E−02	4.87E−03	−5.989	***	
isH4:isJul	−5.50E−02	4.87E−03	−11.277	***	
isH5:isJul	−7.81E−02	4.87E−03	−16.024	***	
isH6:isJul	−1.07E−01	4.87E−03	−21.898	***	
isH7:isJul	−1.47E−01	4.87E−03	−30.174	***	
isH8:isJul	−1.16E−01	4.87E−03	−23.745	***	
isH9:isJul	−4.88E−02	4.87E−03	−10.005	***	
isH10:isJul	1.22E−02	4.87E−03	2.506	*	
isH11:isJul	6.73E−02	4.87E−03	13.805	***	
isH12:isJul	1.15E−01	4.87E−03	23.651	***	
isH13:isJul	1.55E−01	4.87E−03	31.861	***	
isH14:isJul	1.88E−01	4.87E−03	38.54	***	
isH15:isJul	2.13E−01	4.87E−03	43.667	***	
isH16:isJul	2.22E−01	4.87E−03	45.468	***	
isH17:isJul	1.95E−01	4.87E−03	39.986	***	
isH18:isJul	1.15E−01	4.87E−03	23.547	***	
isH19:isJul	7.52E−02	4.87E−03	15.427	***	
isH20:isJul	5.39E−02	4.87E−03	11.066	***	
isH21:isJul	5.97E−02	4.87E−03	12.257	***	
isH22:isJul	8.66E−02	4.87E−03	17.777	***	
isH23:isJul	8.02E−02	4.87E−03	16.449	***	
isH24:isJul	6.22E−02	4.87E−03	12.759	***	
isH1:isAug	−1.64E−02	4.46E−03	−3.688	***	
isH2:isAug	−4.53E−02	4.46E−03	−10.169	***	
isH3:isAug	−7.26E−02	4.46E−03	−16.293	***	
isH4:isAug	−9.68E−02	4.46E−03	−21.728	***	
isH5:isAug	−1.18E−01	4.46E−03	−26.52	***	
isH6:isAug	−1.39E−01	4.46E−03	−31.26	***	
isH7:isAug	−1.75E−01	4.46E−03	−39.168	***	
isH8:isAug	−1.58E−01	4.46E−03	−35.389	***	
isH9:isAug	−9.60E−02	4.46E−03	−21.55	***	
isH10:isAug	−3.73E−02	4.46E−03	−8.371	***	
isH11:isAug	1.68E−02	4.46E−03	3.768	***	
isH12:isAug	6.48E−02	4.46E−03	14.53	***	
isH13:isAug	1.05E−01	4.46E−03	23.497	***	
isH14:isAug	1.38E−01	4.46E−03	30.883	***	
isH15:isAug	1.63E−01	4.46E−03	36.456	***	
isH16:isAug	1.70E−01	4.46E−03	38.225	***	
isH17:isAug	1.42E−01	4.46E−03	31.877	***	
isH18:isAug	6.01E−02	4.46E−03	13.488	***	
isH19:isAug	1.88E−02	4.46E−03	4.216	***	
isH20:isAug	3.67E−03	4.46E−03	0.824		
isH21:isAug	2.65E−02	4.46E−03	5.954	***	

Table A.2 (*continued*)

Variable	Estimate	Std. Error	*t* Value	Significance	Notes
isH22:isAug	3.20E−02	4.46E−03	7.176	***	
isH23:isAug	1.96E−02	4.46E−03	4.398	***	
isH24:isAug	2.70E−03	4.46E−03	0.605		
isH1:isSep	−2.98E−02	4.46E−03	−6.696	***	
isH2:isSep	−5.31E−02	4.46E−03	−11.917	***	
isH3:isSep	−7.32E−02	4.46E−03	−16.425	***	
isH4:isSep	−9.03E−02	4.46E−03	−20.256	***	
isH5:isSep	−1.04E−01	4.46E−03	−23.34	***	
isH6:isSep	−1.09E−01	4.46E−03	−24.482	***	
isH7:isSep	−1.07E−01	4.46E−03	−23.93	***	
isH8:isSep	−1.01E−01	4.46E−03	−22.575	***	
isH9:isSep	−5.78E−02	4.46E−03	−12.966	***	
isH10:isSep	−1.44E−02	4.46E−03	−3.23	**	
isH11:isSep	2.45E−02	4.46E−03	5.495	***	
isH12:isSep	5.76E−02	4.46E−03	12.923	***	
isH13:isSep	8.66E−02	4.46E−03	19.439	***	
isH14:isSep	1.12E−01	4.46E−03	25.06	***	
isH15:isSep	1.30E−01	4.46E−03	29.233	***	
isH16:isSep	1.35E−01	4.46E−03	30.333	***	
isH17:isSep	1.07E−01	4.46E−03	23.973	***	
isH18:isSep	2.60E−02	4.46E−03	5.827	***	
isH19:isSep	−6.25E−03	4.46E−03	−1.402		
isH20:isSep	2.16E−02	4.46E−03	4.85	***	
isH21:isSep	3.75E−02	4.46E−03	8.426	***	
isH22:isSep	2.60E−02	4.46E−03	5.833	***	
isH23:isSep	6.89E−03	4.46E−03	1.546		
isH24:isSep	−1.38E−02	4.46E−03	−3.092	**	
isH1:isOct	−1.58E−02	4.39E−03	−3.603	***	
isH2:isOct	−3.01E−02	4.37E−03	−6.88	***	
isH3:isOct	−4.09E−02	4.39E−03	−9.321	***	
isH4:isOct	−4.90E−02	4.39E−03	−11.16	***	
isH5:isOct	−5.29E−02	4.39E−03	−12.041	***	
isH6:isOct	−4.45E−02	4.39E−03	−10.139	***	
isH7:isOct	−2.13E−02	4.39E−03	−4.856	***	
isH8:isOct	−7.67E−03	4.39E−03	−1.747	.	
isH9:isOct	1.05E−02	4.39E−03	2.385	*	
isH10:isOct	2.83E−02	4.39E−03	6.433	***	
isH11:isOct	4.42E−02	4.39E−03	10.054	***	
isH12:isOct	5.69E−02	4.39E−03	12.957	***	
isH13:isOct	6.84E−02	4.39E−03	15.579	***	
isH14:isOct	7.81E−02	4.39E−03	17.787	***	
isH15:isOct	8.38E−02	4.39E−03	19.08	***	
isH16:isOct	8.03E−02	4.39E−03	18.285	***	
isH17:isOct	5.32E−02	4.39E−03	12.111	***	
isH18:isOct	−9.08E−03	4.39E−03	−2.068	*	
isH19:isOct	6.64E−03	4.39E−03	1.512		
isH20:isOct	3.95E−02	4.39E−03	9	***	
isH21:isOct	3.66E−02	4.39E−03	8.328	***	
isH22:isOct	2.86E−02	4.39E−03	6.518	***	
isH23:isOct	1.45E−02	4.39E−03	3.31	***	
isH24:isOct	−1.47E−04	4.39E−03	−0.034		
isH1:isNov	2.60E−03	4.49E−03	0.58		
isH2:isNov	−4.65E−03	4.48E−03	−1.038		
isH3:isNov	−8.86E−03	4.49E−03	−1.974	*	
isH4:isNov	−1.12E−02	4.49E−03	−2.498	*	
isH5:isNov	−9.79E−03	4.49E−03	−2.182	*	
isH6:isNov	−1.49E−03	4.49E−03	−0.332		
isH7:isNov	5.94E−03	4.49E−03	1.322		
isH8:isNov	7.00E−03	4.49E−03	1.56		
isH9:isNov	2.09E−02	4.49E−03	4.651	***	
isH10:isNov	2.85E−02	4.49E−03	6.359	***	
isH11:isNov	3.29E−02	4.49E−03	7.317	***	
isH12:isNov	3.69E−02	4.49E−03	8.21	***	
isH13:isNov	4.02E−02	4.49E−03	8.947	***	
isH14:isNov	4.31E−02	4.49E−03	9.593	***	
isH15:isNov	4.51E−02	4.49E−03	10.055	***	
isH16:isNov	4.61E−02	4.49E−03	10.274	***	
isH17:isNov	5.34E−02	4.49E−03	11.902	***	
isH18:isNov	5.26E−02	4.49E−03	11.725	***	
isH19:isNov	3.96E−02	4.49E−03	8.821	***	
isH20:isNov	3.56E−02	4.49E−03	7.937	***	
isH21:isNov	3.16E−02	4.49E−03	7.04	***	
isH22:isNov	2.63E−02	4.49E−03	5.866	***	
isH23:isNov	1.96E−02	4.49E−03	4.367	***	
isH24:isNov	1.17E−02	4.49E−03	2.606	**	
isH1:isDec	6.70E−02	6.10E−03	10.989	***	

Table A.2 (*continued*)

Variable	Estimate	Std. Error	*t* Value	Significance	Notes
isH2:isDec	5.89E−02	6.10E−03	9.648	***	
isH3:isDec	5.42E−02	6.10E−03	8.888	***	
isH4:isDec	5.22E−02	6.10E−03	8.562	***	
isH5:isDec	5.19E−02	6.10E−03	8.504	***	
isH6:isDec	5.17E−02	6.10E−03	8.474	***	
isH7:isDec	4.89E−02	6.10E−03	8.014	***	
isH8:isDec	4.92E−02	6.10E−03	8.062	***	
isH9:isDec	5.66E−02	6.10E-03	9.27	***	
isH10:isDec	5.94E−02	6.10E−03	9.731	***	
isH11:isDec	5.78E−02	6.10E−03	9.474	***	
isH12:isDec	5.65E−02	6.10E−03	9.261	***	
isH13:isDec	5.60E−02	6.10E−03	9.173	***	
isH14:isDec	5.63E−02	6.10E−03	9.236	***	
isH15:isDec	5.87E−02	6.10E−03	9.629	***	
isH16:isDec	6.36E−02	6.10E−03	10.424	***	
isH17:isDec	8.52E−02	6.10E−03	13.959	***	
isH18:isDec	9.40E−02	6.10E−03	15.415	***	
isH19:isDec	8.29E−02	6.10E−03	13.583	***	
isH20:isDec	8.25E−02	6.10E−03	13.517	***	
isH21:isDec	8.52E−02	6.10E−03	13.966	***	
isH22:isDec	8.88E−02	6.10E−03	14.562	***	
isH23:isDec	8.88E−02	6.10E−03	14.552	***	
isH24:isDec	8.01E−02	6.10E−03	13.127	***	
isFeb:sun.hours	−9.87E−04	6.10E−05	−16.182	***	
isMar:sun.hours	−1.26E−03	5.75E−05	−21.895	***	
isApr:sun.hours	−1.08E−03	5.84E−05	−18.453	***	
isMay:sun.hours	−3.01E−04	6.44E−05	−4.669	***	
isJun:sun.hours	2.72E−03	1.42E−04	19.115	***	
isJul:sun.hours	−1.60E−03	8.11E−05	−19.676	***	
isAug:sun.hours	−2.11E−04	5.98E−05	−3.536	***	
isSep:sun.hours	−2.08E−04	5.90E−05	−3.519	***	
isOct:sun.hours	−7.26E−04	5.78E−05	−12.549	***	
isNov:sun.hours	−1.03E−03	6.69E−05	−15.318	***	
isDec:sun.hours	−2.88E−03	1.92E−04	−14.989	***	

Note: Dependent variable is residuals from the long-term trend regression (see main paper, step 1). Significance codes: '·' ($P<1$), '.'($P<0.1$).
*** ($P<0.001$).
** ($P<0.01$).
* ($P<0.05$).

Table A.3
Temperature calculations.

$$Tmax_D = max\ Tadj_i \quad \forall\ i \in D$$
$$Tmin_D = min\ Tadj_i \quad \forall\ i \in D \tag{A.1}$$

$$Tmax.\ HDD = max(69\text{–}Tmax_D, 0)$$
$$Tmax.\ CDD = max(Tmax_D - 69, 0)$$
$$Tmin.\ HDD = max(45\text{–}Tmin_D, 0)$$
$$Tmin.\ CDD = max(Tmin_D\text{–}45, 0) \tag{A.2}$$

i = hour of the day
D = day of the year
$Tadj_i$ = hourly adjusted temperature
$Tmax_D$, $Tmin_D$ = daily max and min temperature [°F]

procurement, while still maintaining levels of reliability accepted by other systems. If PJM were to switch to either standard, the 11 GW of coal capacity "at high risk" of retirement could be retired without needing to be replaced. In addition, we find that a reserve margin of 13–15% minimizes total system costs.

PJM's resource adequacy modeling assumes that generator outages are independent. We find that correlated outages among generators could significantly increase outage risk, and cause PJM to underestimate this risk. Evidence suggests that correlated outages do occur with some regularity; winter storms in January 2014 led to 19 GW of natural gas plants and 21 GW of other capacity simultaneously experiencing forced outages (PJM, 2014c). Although winter supply risks have recently been the focus of much attention, we demonstrate that other types of correlated failures may also pose risks. For example, the risk of a forced shutdown of all nuclear generators, while unlikely, could significantly affect reliability.

System operators should be aware that the risk posed by supply shortages is primarily due to extremely severe, but infrequent outages. Our simulations show that the largest 10% of supply shortages are responsible for 50% of unserved energy. Taking into account the possibility of correlated generator outages further exacerbates this risk. The risk of very large outages increases at low reserve margins, suggesting that PJM's policy of over-procuring capacity may be justified.

5. Conclusions and policy implications

Improved understanding of supply shortage risks is increasingly important in today's era of declining reserve margins and coal retirements. Several ISOs, including PJM, have begun to take steps to address these concerns. PJM recently submitted a proposal to the Federal Energy Regulatory Commission (FERC) to establish a Capacity Performance product (PJM, 2014d) that would provide stronger incentives for generators to be available during peak-demand periods.

Resource adequacy modeling is difficult due to the inherent uncertainty intohe likelihood and magnitude of supply shortages. The difficult of resource adequacy modeling is further complicated by the myriad of metrics with which reliability can be measured. NERC recommends that system operators adopt a reliability metric based on unserved energy. We agree. The LOLE metric is flawed, in that it measures only the probability of an outage occurring and ignores both the severity and duration of outages. Our modeling shows that the severity and duration of outage events vary greatly (Table 9), undermining the usefulness of the LOLE metric. Our results also indicate that the 0.1 LOLE standard results in higher reserve margins than other commonly used metrics, such as 0.001% UE or 2.4 LOLH. In 2010, switching from the LOLE standard to a UE or LOLH standard would have allowed PJM to reduce reserve margins from 20.5% to 13%, while maintaining current risk preferences and levels of reliability accepted by other systems. Because supply shortages could cause political fallout both regionally and for system operators, we recommend that ISOs work with NERC and stakeholders to identify both the appropriate UE target and the risk tolerance of PJM participants.

Basing capacity decisions on traditional reliability standards ignores the cost effectiveness of carrying excess capacity. Achieving a very high reliability standard may be possible, but extremely costly. Recently, system operators such as ERCOT have begun to incorporate the cost effectiveness metrics into decision making processes (Newell et al., 2014). A study commissioned by the Public Utility Commission of Texas found that the economically optimal reserve margin in the ERCOT system is 10.2% (Newell et al., 2014). This is lower than the 14.1% reserve margin the study found was needed to meet the 0.1 LOLE study, but higher than the 9.1% reserve margin needed to meet 2.4 LOLH standard and the 9.4% reserve margin needed to meet the 0.001% UE standard. We find that a reserve margin of 13–15% would have minimized total long-term system costs in PJM.

System planners should consider the risks posed by events that can cause correlated outages among generators. Many potential systemic risks exist, including extreme weather, natural disasters, and unforeseeable and sudden regulatory actions that force many plants offline (a risk that was exposed when the Japanese nuclear fleet was shutdown after the Fukushima disaster). Resource adequacy models typically assume plant failures are uncorrelated with one another and therefore ignore systemic risks. We demonstrate that systemic risks may pose a real threat to resource adequacy.

We recommend four specific improvements to the resource adequacy modeling and decision making process.

First, our modeling supports NERC's recommendation that systems move from a LOLE metric of resource adequacy to the unserved energy (UE) metric, which more accurately quantifies the risks of supply shortages. We show that the 0.1 LOLE standard is also conservative compared to the 0.001% UE standard. We find that in 2010 PJM could have reduced reserve margins by 7.5%, or 11 GW, and achieved the 0.001% UE standard used by other systems. System operators should work with stakeholders and NERC to identify what unserved energy targets are appropriate.

Second, we recommend that system operators consider the system cost consequences of resource adequacy decisions. We recommend that PJM and other system operators supplement their resource adequacy modeling and decision making by calculating the economically optimal reserve margin that minimizes total system costs. The results of this analysis should be conveyed to stakeholders and inform capacity procurement decisions alongside traditional reliability metrics.

Third, we recommend further research into systemic risks that can cause many generators to fail at the same time, especially low probability, high impacts risks that are difficult to quantify with retrospective analyses. Our analysis suggests such systemic risks have the potential to negatively affect reliability. These risks are not accounted for in traditional system planning. Additional research is needed into the potential causes of correlated outages, their likelihood, and potential severity. If systemic risks are found to be significant when added to resource adequacy models, systems may need to increase reserve margins.

Finally, the resource adequacy modeling and decision making process should be made more transparent. The methods used should be made publically available. To the extent possible, data and results should also be made publically available. Models should be run under a variety of scenarios and assumptions to test for robustness. The limitations of the modeling should be acknowledged and conveyed to stakeholders and the public.

6. Conflict of interest

The authors declare no competing financial interest.

Acknowledgments

The authors acknowledge support from the Doris Duke Charitable Foundation, the Richard King Mellon Foundation, The Heinz Endowments, and the Carnegie Mellon Electricity Industry Center. This research was also supported in part by the Climate and Energy Decision Making (CEDM) center, created through a cooperative agreement between the National Science Foundation (SES-0949710) and Carnegie Mellon University. This research was also supported by the U.S. Department of Energy's National Energy Technology Laboratory. The authors thank Kathleen Spees for helpful discussions. The views expressed in this paper are strictly those of the authors and do not necessarily state or reflect the views of Carnegie Mellon University or The Brattle Group, Inc.

Appendix A

See Appendix Figs. A.1–A.9 and Tables A.1–A.3.

Detailed regression results

Table A.2 provides detailed regression results for the PJM Classic region. We find that the significant results have the expected sign in most cases. For example, signs are negative for holidays, reflecting that load ar

e lower on these days. Signs are also negative for low-load hours during the night and positive for high-load hours during the day and evening.

Linear model results

We use a non-parametric, additive model to account for the relationship between adjusted average daily temperature and hourly load (see Section 2 – Step 2). However, we also investigated the potential of using a linear model to account for the relationship. As discussed below, we found that using a linear fit worked well for the majority of hours, but considerably over-predicted loads during high temperature days. This over prediction led to the linear model over-estimating the probability of a supply shortage.

The linear model we used in the second step considered the maximum and minimum daily temperature, as shown in Eq. (A.1). We divided days into heating degree days (HDD) and cooling degree days (CDD), as is common in literature (A.2). The split

temperature between HDD/CDD was set to minimize model error: for Tmax terms, the temperature was 20.6 °C. For Tmin terms, temperature was 7.2 °C. We then used a linear and quadratic term for both HDD and CDD temperatures in the regression (A.3).

$$\begin{aligned}\beta_t &= \gamma_1 weekday + \gamma_2(hour{*}month) + \gamma_3 holidays + \gamma_4 T\,max \\ &\quad . HDD + \gamma_5 Tmax.\ CDD + \gamma_6 Tmin.\ HDD + \gamma_7 Tmin.\ CDD \\ &\quad + \gamma_8 Tmax.\ HDD^2 + \gamma_9 Tmax.\ CDD^2 + \gamma_{10} Tmin.\ HDD^2 \\ &\quad + \gamma_{11} Tmin.\ CDD^2 + \gamma_{12}(daylightHours{*}month) + \gamma_t \end{aligned} \quad (A.3)$$

References

Billington, R., Ringlee, R., Wood, A., 1973. Power-System Reliability Calculations. MIT Press.

Bresler, S., PJM, 2012. Personal communication.

Eastern Interconnection States' Planning Council (EISPC), 2013. The Economic Ramifications of Resource Adequacy White Paper. Available at: ⟨http://www.naruc.org/grants/Documents/Economics%20of%20Resource%20Adequacy%20White Paper_Astrape_Final.pdf⟩. (accessed September 2014).

Energy Information Agency (EIA), 2008. Annual Energy Outlook reports, 1999–2008. Available at: ⟨http://www.eia.gov/forecasts/aeo/archive.cfm⟩. Accessed August 2014.

Energy Information Agency (EIA), 2014. Annual Energy Outlook 2014 Early Release. Available at: ⟨http://www.eia.gov/forecasts/aeo/er/index.cfm⟩. (accessed July 2014).

Energy Information Agency (EIA), 2014b. Electricity Data Browser. ⟨http://www.eia.gov/electricity/data/browser⟩ (accessed August 2014).

Hagan, M.T., Behr, S.M., 1987. The time series approach to short term load forecasting. IEEE Trans. Power Syst. 2 (3), 785–791.

Hastie, T, 2013. Package "gam" documentation. Available at: ⟨http://cran.r-project.org/web/packages/gam/gam.pdf⟩ (accessed January 201).

Hines, P., Apt, J., Talukdar, S., 2009. Large blackouts in North America: historical trends and policy implications. Energy Policy 37 (12), 5249–5259.

Hippert, H.S., Pedreira, C.E., Souza, R.C., 2001. Neural networks for short-term load forecasting: a review and evaluation. IEEE Trans. Power Syst. 16 (1), 44–55.

Joskow, P., 2006. Competitive electricity markets and investment in new generating capacity. AEI-Brookings Joint Center Working Paper (06-14).

Joskow, P., 2008. Capacity payments in imperfect electricity markets: need and design. Util. Policy 16 (3), 159–170.

Lazard, 2010. Levelized Cost of Energy Analysis – Version 4.0. ⟨http://webapp.psc.state.md.us/intranet/casenum/NewIndex3_VOpenFile.cfm?filepath=C:%5CCasenum%5C9200-9299%5C9214%5CItem_119%5C%5CSierra%20Club%20and%20CCAN_Case%209214_Supplemental%20Exhibits%20to%20Comments%5CLAZARD%20LCOE%206-12-10.pdf⟩ (accessed August 2015).

Newell, S.A., Spees, K., Pfeifenberger, J., Karkatsouli, I., 2014. Estimating the Economically Optimal Reserve Margin in ERCOT. Prepared for the Public Utility Commission of Texas. Available at: ⟨http://brattle.com/system/news/pdfs/000/000/613/original/Estimating_the_Economically_Optimal_Reserve_Margin_in_ERCOT.pdf?1391445083⟩ (accessed November 2014).

North American Electric Reliability Corporation (NERC), 2010. Final Report on Methodologies and Metrics - September and December, 2010 with Approvals and Revisions. Available at: ⟨http://www.nerc.com/comm/PC/Reliability%20Assessment%20Subcommittee%20RAS%20DL/GTRPMTF_Meth__Metrics_Report_final_w%20_PC_approvals_revisions_12%2008%2010.pdf⟩ (accessed July 2014).

North American Electric Reliability Corporation (NERC), 2014. Generator Availability Data System. Available at: ⟨http://www.nerc.com/pa/RAPA/gads/Pages/default.aspx⟩ (accessed August 2014).

Pfeifenberger, J., Spees, K., Carden, K., Wintermantel, N., 2013. Resource Adequacy Requirements: Reliability and Economic Implications. Available at: ⟨https://www.ferc.gov/legal/staff-reports/2014/02-07-14-consultant-report.pdf⟩ (accessed September 2014).

PJM Interconnection, 2003. PJM Generation Adequacy Analysis: Technical Methods. Available at: ⟨http://www.pjm.com/~/media/etools/oasis/references/white paper-sections-12.ashx⟩ (accessed September 2014).

PJM Interconnection, 2008. 2010/2011 RPM Base Residual Auction Results. Available at: ⟨http://www.pjm.com/~/media/markets-ops/rpm/rpm-auction-info/20080201-2010-2011-bra-report.ashx⟩ (accessed July 2014).

PJM Interconnection, 2009. 2012/2013 RPM Base Residual Auction Results. Available at: ⟨http://www.pjm.com/~/media/markets-ops/rpm/rpm-auction-info/2012-13-base-residual-auction-report-document-pdf.ashx⟩ (accessed June 2014).

PJM Interconnection, 2010a. 2010 PJM Reserve Requirement Study. Available at: ⟨http://www.pjm.com/~/media/documents/reports/2010-pjm-reserve-requirement-study.ashx⟩ (accessed July 2014).

PJM Interconnection, 2010b. EIA 411 Report. Available at: ⟨http://www.pjm.com/documents/reports/eia-reports.aspx⟩ (accessed June 2014).

PJM Interconnection, 2011a. 2010 State of the Market Report for PJM, Volume 2. Available at: ⟨http://www.monitoringanalytics.com/reports/pjm_state_of_the_market/2010/2010-som-pjm-volume2.pdf⟩ (accessed September 2014).

PJM Interconnection, 2011b. Coal Capacity at Risk of Retirement in PJM: Potential Impacts of the Finalized EPA Cross State Air Pollution Rule and Proposed National Emissions Standards for Hazardous Air Pollutants. Available at: ⟨http://pjm.com/~/media/documents/reports/20110826-coal-capacity-at-risk-for-retirement.ashx⟩ (accessed July 2014).

PJM Interconnection, 2013. PJM Manual 19: Load Forecasting and Analysis, Revision 23. Available at: ⟨http://www.pjm.com/~/media/documents/manuals/m19.ashx⟩ (accessed September 2014).

PJM Interconnection, 2014a. Historical Metered Load Data. Available at: ⟨http://www.pjm.com/markets-and-operations/ops-analysis/historical-load-data.aspx⟩ (accessed June 2014).

PJM Interconnection, 2014b. PJM Monthly EFORd Data. Available at: ⟨http://www.pjm.com/markets-and-operations/energy/real-time/historical-bid-data/eford.aspx⟩ (accessed June 2014).

PJM Interconnection, 2014c. Analysis of Operational Events and Market Impacts During the January 2014 Cold Weather Events. Available at: ⟨http://www.pjm.com/~/media/documents/reports/20140509-analysis-of-operational-events-and-market-impacts-during-the-jan-2014-cold-weather-events.ashx⟩ (accessed November 2014).

PJM Interconnection, 2014d. Reforms to the Reliability Pricing Market ("RPM") and Related Rules in the PJM Open Access Transmission Tariff ("Tariff") and Reliability Assurance Agreement Among Load Serving Entities ("RAA"). Submitted to FERC, Docket No. ER15-623-000. Available at: ⟨http://www.pjm.com/~/media/documents/ferc/2014-filings/20141212-er15-623-000.ashx⟩ (accessed January 2015).

PJM Interconnection, 2014e. Scarcity Pricing. Available at: ⟨http://www.pjm.com/~/media/about-pjm/newsroom/fact-sheets/shortage-pricing-fact-sheet.ashx (2014)⟩ (accessed August 2014).

PJM Interconnection, 2014f. Day-Ahead Scheduling Reserve Preliminary Billing Data. Available at: ⟨http://www.pjm.com/markets-and-operations/market-settlements/preliminary-billing-reports/dsr-pjm.aspx⟩ (accessed August 2014).

Spees, K., Newell, S.A., Carlton, R., Zhou, B., Pfeifenberger, J., 2011. Cost of New Entry Estimates For Combustion Turbine and Combined-Cycle Plants in PJM.

Spees, K., Newell, S., Pfeifenberger, J., 2013. Capacity markets-lessons learned from the first decade. Econ. Energy Environ. Policy 2 (2).

Sullivan, Michael J., 2009. Estimated Value of Service Reliability for Electric Utility Customers in the United States. Lawrence Berkeley National Laboratory (accessed September 2014).

U.S. Environmental Protection Agency (EPA), 2014. ⟨http://www.epa.gov/cleanenergy/energy-resources/egrid/index.html⟩ (accessed August 2014).

U.S. National Oceanic and Atmospheric Administration (NOAA), 2013. NWS Windchill Chart. Available at: ⟨http://www.nws.noaa.gov/os/windchill/index.shtml⟩ (accessed August 2014).

U.S. National Oceanic and Atmospheric Administration (NOAA), 2014a. National Climatic Data Center website. Available at: ⟨http://cdo.ncdc.noaa.gov/pls/plclimprod/poemain.accessrouter?datasetabbv=DS3505⟩ (accessed June 2014).

U.S. National Oceanic and Atmospheric Administration (NOAA), 2014b. NWS Weather Service Heat Index. Available at: ⟨http://nws.noaa.gov/os/heat/index.shtml⟩ (accessed August 2014).

U.S. Naval Observatory, 2012. Duration of Daylight/Darkness Table for One Year. Available at: ⟨http://aa.usno.navy.mil/data/docs/Dur_OneYear.php⟩ (accessed June 2014).